haematologica
Journal of the Ferrata Storti Foundation

Co-mutation signatures are age-dependent and impact the prognosis in *NPM1*-mutated acute myeloid leukemia: a PETHEMA multicenter study

by José Vicente Gil, Claudia Sargas, Rosa Ayala, Norma Carmen Gutiérrez, José Antonio Pérez-Simón, María Teresa Gómez-Casares, María José Larrayoz, Esther Prados-de la Torre, Isabel Cano-Ferri, Irene Navarro, Cristina Gil, Teresa Bernal, Eduardo Rodríguez-Arbolí, Esther Pérez-Santaolalla, Rafael Colmenares, Mar Tormo, Juan Bergua, María Luz Amigo, Carlos Rodríguez-Medina, Josefina Serrano, Ana Yurena Oliva, Juan Manuel Alonso-Domínguez, Victor Noriega, Lorenzo Algarra, Mayte Olave, María José García-Pérez, Carmen Couto, Ágata Almela, María García-Fortes, María Dolores Madrigal, María Lourdes Hermosín, Mercedes Colorado, Raimundo García-Boyero, Francisco Ibáñez, María Solé, Carmen Martínez-Chamorro, María del Carmen Mateos, María del Carmen García-Garay, Antonio Solana-Altabella, Beatriz Martín-Herreros, Joaquín Martínez-López, María del Carmen Chillón, Elena Soria, Cristina Bilbao, María José Calasanz, Joaquín Sánchez-García, Eva Barragán and Pau Montesinos

Received: July 7, 2026.
Accepted: July 3, 2026.

Citation: José Vicente Gil, Claudia Sargas, Rosa Ayala, Norma Carmen Gutiérrez, José Antonio Pérez-Simón, María Teresa Gómez-Casares, María José Larrayoz, Esther Prados-de la Torre, Isabel Cano-Ferri, Irene Navarro, Cristina Gil, Teresa Bernal, Eduardo Rodríguez-Arbolí, Esther Pérez-Santaolalla, Rafael Colmenares, Mar Tormo, Juan Bergua, María Luz Amigo, Carlos Rodríguez-Medina, Josefina Serrano, Ana Yurena Oliva, Juan Manuel Alonso-Domínguez, Victor Noriega, Lorenzo Algarra, Mayte Olave, María José García-Pérez, Carmen Couto, Ágata Almela, María García-Fortes, María Dolores Madrigal, María Lourdes Hermosín, Mercedes Colorado, Raimundo García-Boyero, Francisco Ibáñez, María Solé, Carmen Martínez-Chamorro, María del Carmen Mateos, María del Carmen García-Garay, Antonio Solana-Altabella, Beatriz Martín-Herreros, Joaquín Martínez-López, María del Carmen Chillón, Elena Soria, Cristina Bilbao, María José Calasanz, Joaquín Sánchez-García, Eva Barragán and Pau Montesinos. Co-mutation signatures are age-dependent and impact the prognosis in NPM1-mutated acute myeloid leukemia: a PETHEMA multicenter study.
Haematologica. 2026 July 16. doi: 10.3324/haematol.2026.301025 [Epub ahead of print]

Co-mutation signatures are age-dependent and impact the prognosis in *NPM1*-mutated acute myeloid leukemia: a PETHEMA multicenter study

José Vicente Gil[1], Claudia Sargas[1], Rosa Ayala[2], Norma Carmen Gutiérrez[3], José Antonio Pérez-Simón[4], María Teresa Gómez-Casares[5], María José Larrayoz[6], Esther Prados-de la Torre[7], Isabel Cano-Ferri[1,8], Irene Navarro[1,8], Cristina Gil[9], Teresa Bernal[10], Eduardo Rodríguez-Arbolí[4], Esther Pérez-Santaolalla[11], Rafael Colmenares[2], Mar Tormo[12], Juan Bergua[13], María Luz Amigo[14], Carlos Rodríguez-Medina[5], Josefina Serrano[7], Ana Yurena Oliva[15], Juan Manuel Alonso-Domínguez[16], Víctor Noriega[17], Lorenzo Algarra[18], Mayte Olave[19], María José García-Pérez[20], Carmen Couto[21], Ágata Almela[22], María García-Fortes[23], María Dolores Madrigal[24], María Lourdes Hermosín[25], Mercedes Colorado[26], Raimundo García-Boyero[27], Francisco Ibáñez[28], María Solé[29], Carmen Martínez-Chamorro[30], María del Carmen Mateos[31], María del Carmen García-Garay[32], Antonio Solana-Altabella[1,33], Beatriz Martín-Herreros[1], Joaquín Martínez-López[2], María del Carmen Chillón[3], Elena Soria[4], Cristina Bilbao[5], María José Calasanz[6], Joaquín Sánchez-García[7], Eva Barragán[1,34,35,*], Pau Montesinos[1,8,34,*]

1- Grupo Acreditado de Investigación en Hematología, Instituto de Investigación Sanitaria La Fe (IIS La Fe), Valencia, Spain.
2- Hospital Universitario 12 de Octubre, CNIO, Universidad Complutense, Madrid, Spain.
3- Servicio de Hematología, Hospital Universitario de Salamanca (HUS/IBSAL), CIBERONC, Centro de Investigación del Cáncer-IBMCC (USAL-CSIC), Salamanca, Spain.
4- Hospital Universitario Virgen del Rocío, Instituto de Biomedicina (IBIS/CSIC), Universidad de Sevilla, Sevilla, Spain.
5- Hospital Universitario de Gran Canaria Dr. Negrín, Las Palmas de Gran Canaria, Spain.
6- CIMA LAB Diagnostics-Clínica Universidad de Navarra, Pamplona, Navarra Institute for Health Research (IdiSNA), Spain.
7- IMIBIC, Hematology, Hospital Universitario Reina Sofía, UCO, Córdoba, Spain.
8- Servicio de Hematología, Hospital Universitario y Politécnico La Fe, Valencia, Spain.
9- Hospital General Universitario de Alicante, Alicante, Spain.
10- Hospital Universitario Central de Asturias, Instituto Universitario (IUOPA), Instituto de investigación del Principado de Asturias (ISPA), Oviedo, Spain.
11- Hospital Universitario Donostia, Guipúzcoa, Spain.
12- Hospital Clínico Universitario-INCLIVA, Valencia, Spain.
13- Hospital Universitario San Pedro de Alcántara, Cáceres, Spain.
14- Hospital Universitario Morales Messeguer, Murcia, Spain.
15- Hospital Universitario Nuestra Señora de Candelaria, Tenerife, Spain.
16- Hospital Universitario Fundación Jiménez Díaz, Madrid, Spain.
17- Complejo Hospitalario Universitario A Coruña, A Coruña, Spain.
18- Hospital Universitario General de Albacete, Albacete, Spain.
19- Hospital Clínico Universitario Lozano Blesa, Zaragoza, Spain.
20- Complejo Hospitalario Torrecardenas, Almería, Spain.
21- Hospital Virgen de Valme, Sevilla, Spain.
22- Hospital Universitario de León, León, Spain.
23- Hospital Universitario Virgen de la Victoria, Málaga, Spain.
24- Hospital Universitario Virgen de la Macarena, Sevilla, Spain.
25- Hospital General Jerez de la Frontera, Jerez de la Frontera, Cádiz, Spain.
26- Hospital Universitario Marqués de Valdecilla, Santander, Spain.
27- Hospital Universitario General de Castellón, Castellón, Spain.
28- Consorcio Hospital General de Valencia, Valencia, Spain.
29- Hospital Juan Ramón Jiménez, Huelva, Spain.
30- Hospital Universitario Quirón, Madrid, Spain.
31- Complejo Hospitalario de Navarra, Pamplona, Spain.
32- Hospital Universitario Virgen de la Arrixaca, Murcia, Spain.
33- Servicio de Farmacia, Área del Medicamento. Hospital Universitario y Politécnico La Fe, Valencia, Spain.
34- Centro de Investigación Biomédica en Red de Cáncer (CIBERONC), Madrid, Spain.
35- Servicio Análisis Clínicos, Hospital Universitario y Politécnico La Fe, Valencia, Spain.
*Contributed equally

Corresponding authors: Eva Barragán (barragan_eva@gva.es) and José Vicente Gil (jose_gil@iislafe.es)

Conflict of interests: The authors declare no conflict of interests.

Running title: Co-mutations signatures in *NPM1*-mutated AML

Competing Interests

The authors declare no competing financial interests.

Author Contributions

J.V.G wrote the original draft, performed the statistical analysis, and made the figures and tables; C.S., R.A., N.C.G, J.A.P-S., M.T.G-C., M.J.L., E.P-T., A.S-A., B.M-H., J.M-L., M.C.C., E.S., C.B., M.J.C., and J.S-G provided molecular data; I.C-F., I.N., C.G., T.B., E.R-A., E.P-S., R.C., M.T., J.B., M.L.A, C.R-M., J.S., A.Y.O., J.M.A-D., V.N., L.A., M.O., M.J.G-P, C.C., A.A., M.G-F., M.D.M., M.L.H., M.C., R.G-B., F.I., M.S., C.M-C., M.C.M., and M.C.G-G. contributed to patient care and data collection; E.B. and P.M. designed the study and revised the original draft. All the authors critically reviewed and approved the final manuscript.

Data Availability Statement

The datasets used during the current study are available from the PETHEMA AML group coordinator Dr. Pau Montesinos (montesinos_pau@gva.es) on reasonable request.

Acknowledgements

This research was partially funded by the Instituto de Salud Carlos III, Spain: PMP22/00069 and the Scientific Foundation of the Spanish Association Against Cancer to J.V.G. (PRDVA246268GIL).

Abstract

NPM1-mutated acute myeloid leukemia is genetically heterogeneous, and risk assessment remains focused exclusively on *FLT3-ITD* despite the potential role of other co-mutations. We retrospectively analyzed 1,360 adults from a multicenter cohort to map age-resolved co-mutation architecture and prognostic impact. Co-mutations were present in 97% of patients (median = 3 mutations) with *DNMT3A* (45%), *FLT3-ITD* (42%), *TET2* (27%), and *IDH2* (20%) predominating. RTK/RAS partners were enriched in younger adults, whereas myelodysplasia-related genes (MR-genes), epigenetic lesions and higher mutation burden accumulated in the elderly. Pairwise co-mutations mapped to distinct clinical phenotypes with *NPM1+FLT3-ITD* showing a hyperproliferative profile, and *NPM1+SRSF2/TET2* associated to older patients with cytopenic disease. In the 688 patients receiving upfront intensive therapy, *NPM1* type Non-ABD exhibited a tendency toward poorer OS compared with type A. In competing-risk models, *SRSF2* and *DNMT3A* were associated with a higher cumulative incidence of relapse (CIR). Consistently, multivariable analyses showed that increasing age and *SRSF2* independently conferred adverse risk across OS, RFS, and EFS; *KRAS* adversely impacted OS, whereas *FLT3*-OTHER was associated with improved OS; and *DNMT3A* with inferior RFS and EFS but not OS. These findings show that co-mutation signatures in *NPM1*-mutated AML are age-structured and clinically meaningful, refining risk beyond *FLT3*-ITD.

Introduction

Acute myeloid leukemia (AML) is a genetically heterogeneous disease in which recurrent genetic lesions define biologically and clinically distinct subgroups. Among these, *NPM1* mutations are the most frequent in adults (≈30%) and generate an aberrant cytoplasmic protein that enforces HOX/MEIS transcriptional programs and provides a robust marker of measurable residual disease (MRD) [1, 2]. Unlike common age-related clonal hematopoiesis (CH) drivers (e.g., *DNMT3A*, or *TET2*) in AML, *NPM1* variants are virtually absent in CH, consistent with their role as leukemia-initiating events [3]. These molecular and clinicopathologic features anchor *NPM1*-mutated AML in modern diagnostic frameworks and risk adapted treatment [4, 5]. In ELN 2022 stratification, *NPM1*-

mutated with *FLT3*-ITD wild type AML is considered as favorable risk in the absence of adverse cytogenetic, whereas *NPM1*-mutated with *FLT3*-ITD mutated AML (without adverse cytogenetic) is classified as intermediate risk [6]. An open question is whether co-mutations in myelodysplasia-related genes (MR-genes) further modulate the prognostic impact of *NPM1*, particularly within the favorable-risk subset.

Despite this well-established framework, outcomes among patients with *NPM1*-mutated AML remain heterogeneous, suggesting that accompanying lesions shape both disease biology and prognosis. Large series consistently report a median of ~3 co-mutations per case, most commonly involving *DNMT3A*, *FLT3* (ITD/TKD), *IDH1/2*, *PTPN11*, *NRAS*, and *TET2* [7, 8]. Moreover, convergent data indicate that specific combinations portend particularly poor outcomes, such as the *NPM1*+ *DNMT3A*+*FLT3*-ITD triad [9]; whereas others may mitigate risk (e.g., *IDH1/2* or *PTPN11* in selected doublets) [10], underscoring the clinical relevance of interaction patterns rather than single mutations alone. Importantly, both the distribution and prognostic effects of co-mutations partners seem to be age-dependent, several studies suggest that *DNMT3A* (particularly R882) and *IDH1* are associated with inferior outcomes mainly in younger adults, whereas *IDH2* may confer more favorable associations in older patients [11, 12]. Collectively, these observations indicate that *FLT3*-ITD status alone is insufficient to capture prognostic diversity in *NPM1*-mutated AML and that co-mutation profiles may refine risk beyond current categories. However, comprehensive age-dependent co-mutation architecture within large, uniformly defined *NPM1*-mutated cohorts, and its relationship to clinical, biological features and survival, remains scarce.

Here, we analyze 1,360 adults with *NPM1*-mutated AML from the multicenter PETHEMA (Programa Español de Tratamientos en Hematología) registry, integrating harmonized targeted sequencing across seven reference laboratories with clinical covariates and outcomes. Our aims were to (i) chart age specific and mutation burden specific co-mutation networks, (ii) define co-occurrence and mutual exclusivity patterns, and (iii) test associations with baseline clinical variables and overall survival. By shifting the focus from single gene effects to interaction patterns, we aim to clarify how distinct genetic constellations contribute to phenotypic diversity and prognostic heterogeneity in

NPM1-mutated AML, and to identify combination profiles with potential implications for risk stratification and therapeutic decision-making.

Methods

Study design

This was a retrospective multicenter observational study that included patients with *NPM1*-mutated AML diagnosed in seven reference laboratories. Diagnostic samples underwent local morphological, immunophenotype and cytogenetic studies according to standard procedures. Results were harmonized and centrally recorded in the PETHEMA AML registry (NCT02607059). Analyses were performed on the entire *NPM1*-mutated cohort (n = 1,360) for genomics and clinical-biological associations. Outcome and prognostic analyses were conducted in the intensively treated subset (n = 688).

Patients and inclusion criteria

A total of 1,360 newly diagnosed patients treated with intensive and non-intensive chemotherapy regimens were collected from PETHEMA AML registry from January 2016 to November 2024. Pediatric patients (<18 years) and acute promyelocytic leukemia were excluded. Patients were consecutively enrolled in an unselected manner to ensure real world clinical conditions. Each participating institution obtained ethics approval and informed consent in accordance with the Declaration of Helsinki.

Molecular studies

Molecular analyses at diagnosis or hematological relapse were performed by next-generation sequencing (NGS) following harmonized criteria previously established by the PETHEMA group in 7 central laboratories [13]. NGS panels included at least the following genes: *ASXL1, BCOR, BRAF, CALR, CBL, CEBPA, CSF3R, DNMT3A, ETV6, EZH2, FLT3, GATA2, HRAS, IDH1, IDH2, JAK2, KIT, KRAS, MPL, NPM1, NRAS, PTPN11, RUNX1, SETBP1, SF3B1, SRSF2, STAG2, TET2, TP53, U2AF1, WT1*, and *ZRSR2*. Sequencing quality control required a minimum coverage uniformity

above 85% and a mean read depth of at least 1,000×. Variant reporting followed standardized consensus guidelines: all pathogenic or likely pathogenic variants with a variant allele frequency (VAF) ≥5% were reported, while known hotspot mutations in clinically relevant genes were reported down to 1% VAF.

Statistical analysis

Categorical variables were compared using Fisher's exact test (χ^2 when appropriate). Gene-prevalence differences across age groups were summarized as odds ratios (ORs) with Benjamini–Hochberg–adjusted p values. Age–prevalence trends were modeled using binomial generalized additive models (GAMs, logit link) with penalized smoothing splines to capture potential non-linear relationships between age and mutation prevalence, and 95% confidence intervals were computed from model predictions. Co-mutation structure was assessed using pairwise 2×2 tables with Haldane–Anscombe–corrected ORs, Fisher's p, and continuity-corrected φ. For continuous variable comparisons, Wilcoxon rank-sum tests with Cohen's d effect sizes and BH adjustment (requiring ≥5 "double-mutant" cases) were used. Mutation burden across age groups was tested with Kruskal–Wallis and BH-adjusted Dunn post-hoc contrasts. MRD was centrally assessed after induction in peripheral blood by standardized real-time quantitative PCR for mutant *NPM1* transcripts. MRD positivity was defined as ((*NPM1* copies / *ABL1* copies) × 10^5) ≥1. Overall survival (OS) was defined as the time from diagnosis to death. Relapse-free survival (RFS) was measured from the date of diagnosis until relapse or death, whichever occurred first. Event-free survival (EFS) was calculated from the date of diagnosis until treatment failure, relapse, or death. The cumulative incidence of relapse (CIR) was estimated using Fine–Gray competing-risk models, considering death as a competing event. Cox proportional hazards models were used for univariate and multivariate analyses. Genetic alterations included in the multivariate models were selected based on a univariate $p < 0.1$. Co-mutation triads were analyzed in separate univariable survival models and were not incorporated into the multivariable Cox regression. All analyses were performed in R

software (version 4.4.2), with significance thresholds set at $p < 0.05$ or $p < 0.01$, and plots generated using mgcv, complexHeatmap, and ggplot2 packages.

Results

We analyzed 1,360 adults with *NPM1*-mutated AML. Median age was 64 years (range 18–93) and 52.7% were female. Most cases were de novo (68.2%), 12.5% secondary AML, and 19.3% not available. Baseline laboratory values included a median white blood cells (WBC) of 24.95×10⁹/L (range 0.13–483.24), hemoglobin 8.89 g/dL (range 1.89–15.90), platelets 62.5×10⁹/L (range 0.90–939), and bone marrow blasts 72% (range 1–100). Most patients with available cytogenetics showed a normal karyotype (Table 1). Up-front intensive therapy was administered to 688 patients (50.6%), and this subset was used for survival analyses (Supplemental Table 1). All other analyses were performed in the full *NPM1*-mutated cohort (n=1,360), unless otherwise specified.

Genomic Landscape

A total of 4,862 mutations were identified across 1,360 adults with *NPM1*-mutated AML. Co-mutations were present in 1,322/1,360 (97.2%) patients, with a median of 3 mutations (including *NPM1*) per case (range, 1–8). The mutation-burden distribution was right-skewed with a clear mode at three mutations (496/1,360; 36.5%), followed by four (345; 25.4%), two (197; 14.5%), five (185; 13.6%), six (64; 4.7%), seven (27; 2.0%) and eight (8; 0.6%) mutations per patient (Supplemental Figure 1). Among 1,360 patients, 76.4% (1,039/1,360) carried the type A variant, 6.2% (84/1,360) type B, 6.9% (94/1,360) type D, and 10.5% (143/1,360) were classified as Non-ABD.

The most frequent co-mutations were *DNMT3A* (610; 45%), *FLT3*-ITD (567; 42%), *TET2* (362; 27%), *IDH2* (278; 20%), *IDH1* (205; 15%), *NRAS* (201; 15%), and *SRSF2* (189; 14%) (Figure 1). Grouped by functional classes according to Benard et al. [14], alterations in DNA methylation genes (1112; 81.8%) were the most frequent, followed by RTK/RAS signaling (1011; 74.3%), while tumor suppressors and chromatin/cohesin lesions were infrequent (112; 8.2%–84; 6.2%) (Supplemental Table 2). MR-genes were mutated in 297 (21.8%) patients, of whom 253 (85.2%) patients carried a

single mutation, and 44 (14.8%) had ≥2 mutations. Regarding cytogenetic abnormalities, trisomy 8 was the most frequent recurrent alteration (Supplemental Table 3) and was significantly associated with *DNMT3A* (p = 0.012) and *FLT3*-ITD (p = 0.041).

Among patients with paired diagnostic and relapse samples, 15.4% showed no changes in their mutational profile, whereas 22.1% showed only mutation losses, 25.7% only mutation gains, and 36.8% both losses and gains. Gene-level analysis revealed that *NPM1* was largely stable at relapse, although 12.5% of relapsing patients no longer harbored detectable *NPM1* mutation, indicating relapse from an *NPM1*-negative or ancestral clone in a subset of cases. *DNMT3A* was also predominantly stable, while *FLT3*-ITD and other signaling lesions showed more dynamic patterns, with frequent losses and gains at relapse (Supplemental Figure 2; Supplemental Table 4). When stratified by the number of mutated genes (k), co-mutation networks showed a graded increase in complexity from low mutation burden to dense constellations. Cases with few mutations (k=2–3) were dominated by the classic *NPM1* partners (*DNMT3A*, *FLT3*-ITD, or *IDH1/2*) or additional partners in the RAS/MAPK pathway (e.g., *NRAS*, *PTPN11*). As the mutational burden increased (k≥4), the landscape broadened to include MR-genes/splicing genes (e.g., *SRSF2*, *U2AF1*, *SF3B1*), while *DNMT3A* and *FLT3*-ITD remained central anchors. This pattern suggests stepwise clonal layering, from simple *NPM1*-based genotypes to multi-pathway architectures that may impact treatment response and outcomes.

Clinical features and molecular associations

Patients with type A had higher leukocyte counts compared with Non-ABD cases (median 26×10⁹/L vs 16×10⁹/L; p = 0.0037) and occurred less frequently in younger individuals (≤45 years) (Figure 2A). Genomic associations also differed across *NPM1* types: types A and B were enriched for *DNMT3A* and *IDH2*, and for *PTPN11* and *WT1*, respectively, whereas Non-ABD variants showed a lower frequency of the canonical co-mutations partners *DNMT3A* and *FLT3*-ITD (Figure 2B-C). No significant differences in cytogenetic status were observed across *NPM1* subtypes.

Age-related differences

All patients were distributed in four age groups: ≤45 years (n = 149), 46–60 (n = 386), 61–75 (n = 538), and >75 (n = 287) (Supplemental Figure 3A). Per gene prevalences (Supplemental Figure 3B) and pathway summaries (Supplemental Figure 3C) show that DNA methylation genes are frequent at all ages, *RTK/RAS/MAPK* partners are most represented in younger adults, and splicing/cohesin alterations accumulate with age. Continuous trend modeling (GAM with 95% CIs; Supplemental Figure 4A) identified 12 genes with significant age-related trajectories: *ASXL1, CSF3R, DNMT3A, EZH2, FLT3*-ITD*, FLT3*-OTHER*, FLT3*-TKD*, JAK2, PTPN11, SF3B1, SRSF2*, and *TET2*. A marked age decline was observed in *FLT3*-ITD, *FLT3*-TKD, *PTPN11*, *NRAS*, and *CSF3R*, whereas MR genes (*SRSF2*, *ASXL1*, *SF3B1*), and *TET2* increased with age; the latter displaying a shallow mid-life dip followed by a late rise (Supplemental Table 5; Supplemental Figure 5). *DNMT3A* followed a peaked trajectory with highest prevalence in mid-adult life, and low-frequency kinases such as *JAK2* exhibited a slight uptick in the oldest patients (Supplemental Figure 4B).

The number of mutations increased with age. The means (±SD) were 3.53 ± 1.31, 3.55 ± 1.26, 3.49 ± 1.22, and 4.36 ± 1.24 for the ≤45, 46–60, 61–75, and >75 groups, with ranges of 1–7, 1–8, 1–7, and 2–8, respectively. Although the overall Kruskal–Wallis test did not reach conventional significance ($\chi^2 = 6.08$; $p = 0.082$), BH-adjusted pairwise Wilcoxon tests indicated that the >75 years group carried a higher mutational burden than each younger stratum (adjusted $p = 0.042$). This pattern is consistent with the age-stratified circus plots, where dense, multi-pathway constellations ($k \geq 4$) were observed in 64.4% of >75 years patients versus 40% of those ≤45 (Supplemental Figure 4C).

The distribution of recurrent gene mutations according to cytogenetic status (normal vs altered karyotype) was explored across age groups. *FLT3*-ITD mutations were more frequently observed in patients aged 45–60 and 61–75 years with normal karyotype compared with those with altered cytogenetics (47.9% vs 24.2%, $p = 0.013$; and 41.5% vs 19.6%, $p = 0.003$, respectively). In

contrast, *TP53* mutations were enriched in patients older than 75 years with altered cytogenetics (7.8% vs 2.1%, p = 0.029) (Supplementary Table 6).

Co-mutation patterns

The most reproducible co-occurrences were *DNMT3A*+*FLT3*-ITD, *IDH2*+*SRSF2*, and *NRAS*+*PTPN11*. In contrast, strong mutual exclusivities were observed between *IDH1*+*IDH2*, *TET2* and either *IDH1* or *IDH2*, *DNMT3A*+*SRSF2*, and between *FLT3*-ITD and other RAS/MAPK drivers (*NRAS*, *KRAS*, *PTPN11*). In younger patients presenting *DNMT3A*+*FLT3*-ITD, the mutual exclusivity with other signaling mutations was more apparent, whereas in older adults epigenetic lesions (*DNMT3A/IDH/TET2*) were increasingly connected with MR genes (*SRSF2/SF3B1/U2AF1*), and the *TET2*+*IDH1/2* exclusivity became more pronounced (Supplemental Figure 4D).

In the overall cohort, co-mutated doublets showed distinct presentation phenotypes at diagnosis. Proliferative patterns were seen with signaling partners like *NPM1*+*FLT3-ITD* associated with higher WBC, higher peripheral-blood blasts, and higher LDH; a similar (though slightly milder) leukocytosis was observed for *NPM1*+*DNMT3A*. By contrast, *NPM1*+*SRSF2* and *NPM1*+*TET2*, mapped to older age and lower WBC, while *NPM1*+*DNMT3A* was associated with younger patients. Epigenetic partners showed mixed, generally less proliferative shifts, with *NPM1*+*IDH1* and *DNMT3A*+*IDH1* showing higher platelet counts (Figure 3A). The most frequent three-gene genotype (*NPM1*+*DNMT3A*+*FLT3*-ITD*)* showed a similar pattern as *NPM1*+*FLT3*-ITD with higher WBC and younger age. No significant differences were observed in baseline clinical variables between patients with normal vs altered cytogenetics.

Multi-hit impact

In the overall cohort, we also investigated whether multiple mutations within the same gene (multi-hit) or functional pathway were linked to presentation. Multi-hit *FLT3* (ITD/TKD/OTHER) was associated with older age, and higher hemoglobin and blasts counts ($q < 0.1$), *PTPN11* showed a

strong association with higher bone marrow blasts ($q < 0.1$), and multi-hit *NRAS* was associated with higher platelet counts ($q < 0.3$). Multi-hit *TET2* showed a younger age signal and lower bone marrow blast counts ($q < 0.3$). When collapsing by functional class, DNA-methylation multi-hits were linked to a less proliferative profile at diagnosis and younger age ($q < 0.1$). In contrast, RTK/RAS-signaling multi-hits were associated with a more proliferative presentation (higher blast counts) and older age ($q < 0.1$) (Figure 3B).

Prognostic impact of co-mutations among intensively treated patients

We next restricted analyses to the 688 patients who received up-front intensive therapy to explore how *NPM1* type and pairwise co-mutations shape clinical outcomes. According to ELN 2022 classification, this cohort included 362 (52.6%) favorable, 315 (45.8%) intermediate, and 11 (1.6%) adverse-risk cases. Overall, type Non-ABD showed a trend toward inferior OS compared with type A (HR = 1.43, 95% CI 0.99–2.07; p = 0.059) (Supplemental Figure 6).

Univariate analysis showed poorer OS for *SRSF2* (HR = 1.70, 1.20-2.60, p=0.006), *ETV6* (HR = 2.80, 1.20-6.20, p=0.015), *FLT3*-ITD (HR = 1.40, 1.01-1.80, p=0.020), while *FLT3-OTHER* (non-ITD/TKD) (HR = 0.52, 0.29-0.92, p=0.026) was associated with a favorable outcome (Supplemental Figure 7; Supplemental Table 7). Consistent results were observed for RFS and EFS where *SRSF2* remained associated with inferior RFS (HR = 1.95, 95% CI 1.38–2.74, p < 0.001) and EFS (HR = 1.87, 95% CI 1.34–2.63, p < 0.001), while *ETV6* also conferred adverse RFS (HR = 2.29, 95% CI 1.08–4.85, p = 0.031) and EFS (HR = 2.13, 95% CI 1.00–4.50, p = 0.049). In contrast, *FLT3*-OTHER retained a protective effect on RFS (HR = 0.61, 95% CI 0.38–0.99, p = 0.044), and *NRAS* mutations were associated with improved EFS (HR = 0.69, 95% CI 0.48–0.99, p = 0.045) (Supplemental Tables 8 and 9). Analysis of cumulative incidence of relapse (CIR), accounting for death as a competing risk, further supported these findings, identifying *DNMT3A* (HR = 1.81, 95% CI 1.27–2.58, p < 0.001), *SRSF2* (HR = 1.98, 95% CI 1.21–3.24, p = 0.007), and *CEBPA* (HR = 1.92, 95% CI 1.01–3.64, p = 0.046) as significantly associated with increased relapse risk

(Supplemental Table 10). In the subset of patients with available post-induction MRD data, MRD positivity was associated with significantly inferior OS (HR = 1.72, 1.01-2.93, p = 0.045). Consistently, MRD-positive patients showed a significantly higher CIR (Gray's test p = 0.009), with estimated CIR rates at 1, 2, and 3 years of 23.9%, 32.4%, and 35.5% versus 7.7%, 15.3%, and 21.9%, respectively (Supplemental Figure 8). No significant differences were observed for the competing risk of death without relapse (p = 0.59).

Age-stratified univariate analyses in age-related genes confirmed that these effects were age-restricted: *FLT3*-ITD showed increased adverse prognostic impact in patients aged 61–75 years across OS, RFS, and EFS (HRs 1.52–1.58; p = 0.022), *SRSF2* was associated with inferior outcomes in the same age group for OS, RFS, and EFS (HRs 1.62–1.95; p ≤ 0.04), whereas *FLT3*-OTHER was associated with improved OS and RFS in patients aged 46–60 years (HRs 0.16 and 0.44; p ≤ 0.04). In addition, *DNMT3A* conferred an adverse effect on RFS and EFS specifically in the 46–60-year group (HRs 1.78–1.81; p ≤ 0.006). Detailed results for OS, RFS, and EFS are provided in Supplemental Tables 11–13.

Notably, among *NPM1+FLT3*-ITD patients, those treated with FLT3 inhibitors (FLT3i)—predominantly midostaurin—showed significantly improved OS compared with FLT3i untreated patients (HR = 0.61, 0.43–0.88, p = 0.009) (Supplemental Figure 9). Kaplan-Meier curves for all tested genes are shown in Supplemental Figure 10. We further stratified patients according to *FLT3*-ITD allelic burden as no *FLT3*-ITD, *FLT3*-ITD microclone (<0.05), or *FLT3*-ITD ≥0.05. *FLT3* microclones did not significantly differ from *FLT3*-ITD–negative patients for OS (HR = 1.33; 95% CI, 0.65–2.71; p = 0.44), or FLT3-ITD ≥0.05 cases (HR = 0.90; 95% CI, 0.44–1.85; p = 0.78). For RFS and EFS, *FLT3* microclones showed curves closely overlapping with *FLT3*-ITD ≥0.05, with no significant differences between these two groups (RFS: HR = 1.10; 95% CI, 0.57–2.10; p = 0.78; EFS: HR = 1.05; 95% CI, 0.55–2.00; p = 0.89), suggesting that *FLT3*-ITD microclones may behave similarly to higher-burden *FLT3*-ITD for relapse-related outcomes (Supplemental Figure 11).

Then we explored MR-genes analyzing the number of MR-genes mutations and the type of MR-gene mutated. Among the 688 patients, 17% harbored mutations in MR-genes, most commonly involving *SRSF2* and *ASXL1* (Figure 4A). Overall, 88.2% of MR-positive patients carried a single

mutation, whereas 11.8% had ≥2 mutations. A single MR-gene mutation did not confer a significantly inferior OS (HR = 1.20, 95% CI 0.84–1.71, p = 0.314), although *SRSF2* showed a trend toward adverse outcome (HR = 1.50, 95% CI 0.99–2.30, p = 0.059) (Supplemental Figure 12). In contrast, patients harboring two or more mutations had a significantly poorer survival (HR = 2.42, 95% CI 1.14–5.16, p = 0.022) (Figure 4B). Restricting the analysis to the ELN favorable-risk *NPM1*, MR-genes did not significantly impact OS (HR = 1.35, 95% CI 0.32–5.77, p = 0.681).

We also investigated whether multiple mutations within the same gene or functional pathway were linked to OS. No single gene reached FDR-significance for OS (all $q > 0.3$), but directions were consistent with their clinical profiles: *TET2*, *NRAS*, and *DNMT3A* multi-hits trended toward worse OS (hazard ratio [HR] ≳1.2–1.6), whereas *PTPN11* showed a slight HR <1. Clustering by functional class, DNA-methylation multi-hits were linked to worse OS (HR 1.5; $p=1.5\times10^{-2}$; q=0.05).

We next asked whether three-gene constellations modify prognosis beyond doublets. We evaluated triads that occurred at appreciable frequency (≥10 patients) and estimated their HR against patients carrying the corresponding pairwise background (Supplemental Figure 13A). Overall, the unfavorable spectrum was enriched for triads built on *TET2* and *SRSF2*. *NPM1+TET2+IDH2, NPM1+TET2+SRSF2, NPM1+FLT3*-ITD+*TET2,* and *NPM1+FLT3*-ITD+*SRSF2* were the most frequent triads associated with poorer outcomes and (HRs >1, p < 0.05; q-values 0.1–0.3) (Supplemental Figure 13B and Supplemental Table 14). The triad *NPM1+DNMT3A+FLT3*-ITD was the most frequent and showed a directionally worse HR for OS, RFS and EFS, but did not reach statistical significance either overall or in any age group. However, it was associated with a higher CIR (HR = 1.52, 95% CI 1.04–2.21, p = 0.029), suggesting that this genotype primarily increases relapse propensity rather than mortality. To test whether the *DNMT3A* hotspot was driving risk, we stratified the triad by codon R882 and compared each subgroup with the remainder of the cohort. *NPM1+DNMT3A*^{R882}*+FLT3*-ITD showed poorer outcome (HR = 1.40, 1.00–1.96; p = 0.050) than *NPM1+DNMT3A*$^{non\text{-}R882}$*+FLT3*-ITD (HR = 1.09, 0.68–1.73; p = 0.728), but neither subgroup showed a significant OS difference (p = 0.14) (Supplemental Figure 14A). Additionally, within the

NPM1+DNMT3A+FLT3-ITD subset, patients treated with FLT3i showed a slightly improved OS compared with untreated counterparts (HR = 0.73, 95% CI 0.44–1.19, p = 0.206), suggesting a potential therapeutic benefit (Supplemental Figure 14B). Conversely, several *FLT3*-OTHER and *NRAS*–containing triads trended toward a better survival, in line with the favorable effect observed for these genes as a single partner. This suggests that co-occurrence accentuates the prognosis seen for these genes individually or as doublets (Supplemental Figure 13B).

Finally, multivariate analysis showed that increasing age remained an independent adverse prognostic factor across all endpoints (OS, RFS, and EFS; all p < 0.001). Among genetic variables, *SRSF2* emerged as the most robust adverse factor, independently associated with inferior OS (HR = 1.98, 95% CI 1.15–4.12, p = 0.037), RFS (HR = 2.74, 95% CI 1.43–5.28, p = 0.002), and EFS (HR = 2.74, 95% CI 1.43–5.24, p = 0.002). *KRAS* was associated with inferior OS (HR = 1.96, 95% CI 1.21–3.17, p = 0.006), showing borderline effects for RFS and EFS. In contrast, *FLT3*-OTHER retained a protective effect on OS (HR = 0.60, 95% CI 0.32–0.91, p = 0.010), with consistent trends for RFS and EFS. *DNMT3A* independently conferred an increased risk of relapse and event occurrence, remaining significant for RFS (HR = 1.53, 95% CI 1.16–2.03, p = 0.003) and EFS (HR = 1.47, 95% CI 1.12–1.94, p = 0.006), but not for OS (Table 2). In a second multivariate model restricted to patients with MRD available, MRD positivity was consistently associated with inferior outcomes across all endpoints (Supplemental Table 15).

Discussion

In this study we examined the spectrum of *NPM1* co-mutations and their association with clinical characteristics and patient outcomes in a real-world, multicenter cohort of 1,360 adults (688 treated up-front with intensive therapy). To our knowledge, this series characterized with a harmonized NGS workflow and treated according to the PETHEMA cooperative group recommendations, constitutes the largest *NPM1*-mutated AML cohort analyzed to date. Our data show how the *NPM1* genomic background varies systematically with age and that a small set of co-mutations dominate prognosis in *NPM1* patients.

The mutational landscape was consistent with previous studies where *DNMT3A*, *FLT3*-ITD, *TET2*, and *IDH1/2* were the most common partners. The prevalence of *SRSF2* was higher in our series than in several trial-based series [15, 16], likely due to its age-linkage and the older age distribution of our cohort. In fact, our results show an age-stratified biology with 12 genes varying significantly across age groups. RTK/RAS pathway genes (*FLT3, PTPN11*) were most prevalent in younger adults and waned steadily with advancing age, whereas splicing (*SRSF2*, *SF3B1*) and epigenetic factors (*ASXL1*, *TET2*) accumulated with age. In addition, the number of mutations was strongly associated with aging, the oldest stratum (>75 years) carried more mutations per case and showed denser, multi-pathway constellations, suggesting distinct age associated leukemogenic trajectories where signaling and proliferative programs are dominant in younger patients versus epigenetic/splicing programs in older adults. These observations align with prior studies linking aging to accumulation of CH mutations, higher mutation counts, and worse outcome; and support age-stratified refinement of genetic risk in *NPM1*-mutated AML [17].

The distribution and clinical features of *NPM1* types showed that type A accounted approximately three quarters of all cases, whereas non-A variants (B, D, and Non-ABD) were collectively more frequent in younger adults and displayed distinctive molecular features. Specifically, Non-ABD cases exhibited a lower frequency of the canonical partners *DNMT3A* and *FLT3-ITD* and a trend toward inferior OS compared with type A. This observation is consistent with findings from Othman et al. [18], who also described worse outcomes for Non-ABD variants in an independent large cohort. Although these variants have not been fully characterized, their distinct molecular context may underlie distinct biological behavior. Clinically, *NPM1*-mutated non-ABD cases currently lack standardized molecular MRD assays and are often omitted from MRD-guided treatment protocols. This may further contribute to their less favorable outcomes and underscores the need for harmonized follow-up and therapeutic strategies across all *NPM1* subtypes.

Genotype pairs mapped to distinct presentation phenotypes at diagnosis. As expected, signaling-driven doublets like *NPM1+FLT3-ITD* showed a hyper-proliferative profile with leukocytosis, higher blast counts, and elevated LDH consistent with constitutive RTK/RAS/MAPK activation [19]. In

contrast, combinations with MR-genes and *TET2* clustered in older patients and were associated with lower WBC and broader cytopenias. Notably, doublets involving *IDH1* showed higher platelet counts. A plausible explanation could be that *IDH1* mutations produce 2-hydroxyglutarate, which can reprogram hematopoiesis toward megakaryocytes and cause mild thrombocytosis in some patients [20]. These clinical signatures may help understand the intricate physiopathology underlying the heterogeneous presentation of *NPM1*-mutated patients.

Once demonstrated that co-mutations are age-dependent and drive distinct presentation phenotypes, we assessed the impact on survival after intensive chemotherapy approaches. According to the biology described above, MR-genes that accumulate with age translated into an independent hazard for *SRSF2*. Beyond overall survival, *SRSF2* also consistently conferred an increased risk of relapse and events, remaining independently associated with inferior RFS and EFS and with a higher cumulative incidence of relapse in competing-risk analyses. The proliferative RTK/RAS pathway manifested as adverse risk for *FLT3*-ITD and *KRAS*, although the use of FLT3i appeared to mitigate the negative prognostic impact of *FLT3*-ITD, as treated patients showed a significantly better OS [21]. In contrast, not all *FLT3* alterations behaved alike, while *FLT3*-ITD showed worse survival, *FLT3*-OTHER (non-ITD/TKD) was significantly associated with improved outcome, underscoring that *FLT3* mutations are prognostically heterogeneous in *NPM1*-mutated AML. Finally, *DNMT3A* was primarily associated with relapse-related endpoints, conferring an increased risk of relapse and events (RFS, EFS, and CIR) without an independent impact on OS.

We also revisited the long-standing question regarding the prognostic contribution of MR-genes. Previous studies have reported divergent results, with Wright et al. [22] suggesting mutual exclusivity between MR-genes and *NPM1*, likely influenced by limited cohort size; recent series [15, 16] reporting no clear OS impact; and others reporting adverse outcomes mainly when two or more MR-gene mutations coexisted [23]. These discrepancies may partly reflect differences in study design, certain analyses focused only on clinical trial patients, who tend to be younger and less enriched for MR-gene mutations, or on subsets restricted to ELN 2022–favorable cases.

In our study, we evaluated all *NPM1*-mutated cases and also the ELN 2022 favorable subset separately. Consistent with Lachowiez et al. [23], our results in the entire cohort showed that the presence of two or more MR-gene mutations was associated with inferior OS in univariate analysis but not independently. However, *SRSF2* emerged as a main adverse component in multivariate model, consistent with the findings by Lachowiez et al. [23], who also identified *SRSF2* as the MR-gene most strongly associated with poor prognosis. Moreover, *SRSF2* accounted for nearly half of MR-positive cases and was overrepresented among multi-mutated patients (75% of those with two MR-genes and 100% with ≥3), indicating that the apparent cumulative effect of MR alterations is largely driven by the presence of *SRSF2*. These findings contrast with the recent study by Bill et al. [24], who analyzed a large intensively treated cohort harboring MR-genes and reported better outcome for *SRSF2* compared with other MR-genes. Our results suggest a distinct biological behavior within an *NPM1*-mutated background, and that previously reported MR-burden effects in *NPM1*-mutated AML may be driven by *SRSF2* composition. Collectively, these data highlight the relevance of identifying which MR-gene is mutated rather than how many, particularly in older adults where these lesions are more prevalent. In line with Eckardt et al. [16] and Cocciardi et al. [15], we did not observe an adverse impact of MR-genes on OS within the *NPM1* favorable-risk group.

Moving beyond pairs, triple-mutated genotypes revealed consistent adverse triads layering *TET2* and *SRSF2* onto canonical *NPM1* partners, supporting that MR-genes and epigenetic lesions amplify risk when combined with proliferative drivers. Conversely, triads incorporating *NRAS* or *FLT3-OTHER* were associated with a trend of better survival, mirroring the favorable effect of these single partners in multivariable model. Of note, we did not observe a significant detriment OS for the classic *NPM1*+*DNMT3A*+*FLT3*-ITD triad, even when *DNMT3A* was split into R882 (previously reported as more adverse risk) and non-R882 subsets [25]. These results contrast with previous reports by Hernández-Sánchez et al. [26] and Yao et al. [7]. A plausible explanation is the differential use of selective inhibitors: prior cohorts excluded patients who received FLT3i, whereas in ours up to 57.7% of these patients received FLT3-TKI inhibitors with intensive chemotherapy, suggesting that targeted FLT3 inhibition may attenuate the historical risk associated with this

genotype. Indeed, recent analyses from the Quantum-first trial suggested that patients with this triad could benefit particularly from the addition of quizartinib [27].

This work has limitations inherent to its real-world design. Although sequencing was harmonized across seven reference laboratories, platform and panel updates over time, variant classification, and missingness for some cases (including cytogenetics) could introduce potential heterogeneity. Survival analyses were restricted to the intensively treated subset (n=688), with treatment heterogeneity including the use of FLT3i, which may introduce variability in effect estimates. Nevertheless, given the unselected, consecutive nature of the PETHEMA registry, we do not anticipate a relevant selection bias related to incomplete treatment information. Power was limited for rare genes and infrequent triads despite false-discovery rate control, and we did not assess the effect of allogeneic transplant.

Even with these considerations, several conclusions emerge with direct clinical relevance. Co-mutations in *NPM1*-mutated AML are strongly age-structured and clinically meaningful with *SRSF2, DNMT3A* and *ETV6* carrying adverse risk, and *FLT3*-OTHER showing favorable outcomes. Notably, the adverse effect observed for *ETV6* was limited to univariable analyses and should be regarded as exploratory, given its low frequency and lack of independent significance after multivariable adjustment. The prognostic signal attributed to MR-genes reflects gene identity rather than mutation count, with *SRSF2* driving risk. Given the high prevalence of *SRSF2* in older adults, often ineligible for intensive therapy, and the emergence of SRSF2-directed strategies [28], evaluation of targeted approaches in this population should be considered. In the contemporary FLT3 inhibitor era, the historical hazard of the *NPM1*+*FLT3*-ITD and *NPM1*+*DNMT3A*+*FLT3*-ITD appears attenuated. Beyond the robust observations in this large series, these findings warrant prospective validation in independent cohorts with the integration of MRD metrics, clonal dynamics, and quantitative features such as variant allele frequency. Based on our data, we propose considering co-mutation signatures for risk stratification and treatment selection, particularly as the treatment landscape is constantly evolving with the development of novel inhibitors.

References

1. Falini B. NPM1-mutated acute myeloid leukemia: New pathogenetic and therapeutic insights and open questions. Am J Hemat. 2023;98(9):1452-1464.

2. Christopher MR, Nawas MT, Reagan JL. Molecular measurable residual disease monitoring and transplant indications in NPM1 mutated acute myeloid leukemia. Bone Marrow Transplant. 2025;60(2):135-143

3. McKerrell T, Park N, Moreno T, et al. Leukemia-Associated somatic mutations drive distinct patterns of Age-Related clonal hemopoiesis. Cell Rep. 2015;10(8):1239-1245.

4. Khoury JD, Solary E, Abla O, et al. The 5th edition of the World Health Organization classification of haematolymphoid tumours: myeloid and histiocytic/dendritic neoplasms. Leukemia. 2022;36(7):1703-1719.

5. Arber DA, Orazi A, Hasserjian RP, et al. International Consensus Classification of Myeloid Neoplasms and Acute Leukemias: integrating morphologic, clinical, and genomic data. Blood. 2022;140(11):1200-1228.

6. Döhner H, Wei AH, Appelbaum FR, et al. Diagnosis and management of AML in adults: 2022 recommendations from an international expert panel on behalf of the ELN. Blood. 2022;140(12):1345-1377.

7. Yao Y, Zhou Y, Zhuo N, et al. Co-mutation landscape and its prognostic impact on newly diagnosed adult patients with NPM1-mutated de novo acute myeloid leukemia. Blood Cancer J. 2024;22;14(1):118.

8. Cocciardi S, Weiß N, Saadati M, et al. The genomic landscape and its clinical implication in NPM1-mutated AML patients: a study within the AMLSG 09-09 Clinical trial. Blood. 2023;142(Supplement 1):4311.

9. Bezerra MF, Lima AS, Piqué-Borràs M-R, et al. Co-occurrence of DNMT3A, NPM1, FLT3 mutations identifies a subset of acute myeloid leukemia with adverse prognosis. Blood. 2020;135(11):870-875.

10. Fobare S, Kohlschmidt J, Ozer HG, et al. Molecular, clinical, and prognostic implications of PTPN11 mutations in acute myeloid leukemia. Blood Adv. 2021;6(5):1371-1380.

11. Oñate G, Bataller A, Garrido A, et al. Prognostic impact of DNMT3A mutation in acute myeloid leukemia with mutated NPM1. Blood Adv. 2021;6(3):882-890.

12. Lachowiez CA, Reville PK, Kantarjian H, et al. Contemporary outcomes in IDH-mutated acute myeloid leukemia: The impact of co-occurring NPM1 mutations and venetoclax-based treatment. Am J Hemat. 2022;97(11):1443-1452.

13. Sargas C, Ayala R, Chillón MC, et al. Networking for advanced molecular diagnosis in acute myeloid leukemia patients is possible: the PETHEMA NGS-AML project. Haematologica. 2020;106(12):3079-3089.

14. Benard BA, Leak LB, Azizi A, Thomas D, Gentles AJ, Majeti R. Clonal architecture predicts clinical outcomes and drug sensitivity in acute myeloid leukemia. Nat Commun. 2021;12(1):7244.

15. Cocciardi S, Saadati M, Weiß N, et al. Impact of myelodysplasia-related and additional gene mutations in intensively treated patients with NPM1-mutated AML. Hemasphere. 2025;15;9(1):e70060.

16. Eckardt J-N, Bill M, Rausch C, et al. Secondary-type mutations do not impact outcome in NPM1-mutated acute myeloid leukemia – implications for the European LeukemiaNet risk classification. Leukemia. 2023;37(11):2282-2285.

17. Li J-F, Cheng W-Y, Lin X-J, et al. Aging and comprehensive molecular profiling in acute myeloid leukemia. Proc Natl Acad Sci USA. 2024;121(10):e2319366121.

18. Othman J, Potter N, Ivey A, et al. Molecular, clinical, and therapeutic determinants of outcome in NPM1-mutated AML. Blood. 2024;144(7):714-728.

19. Decroocq J, Birsen R, Montersino C, et al. RAS activation induces synthetic lethality of MEK inhibition with mitochondrial oxidative metabolism in acute myeloid leukemia. Leukemia. 2022;36(5):1237-1252.

20. Veninga A, De Simone I, Heemskerk JWM, Cate HT, Van Der Meijden PEJ. Clonal hematopoietic mutations linked to platelet traits and the risk of thrombosis or bleeding. Haematologica. 2020;105(8):2020-2031.

21. Reville PK, Sasaki K, Kantarjian HM, et al. Improved outcomes among newly diagnosed patients with FMS-like tyrosine kinase 3 internal tandem duplication mutated acute myeloid leukemia treated with contemporary therapy: revisiting the European LeukemiaNet adverse risk classification. Am J Hemat. 2022;97(3):329-337.

22. Wright MF, Pozdnyakova O, Hasserjian RP, et al. Secondary-type mutations do not impact prognosis in acute myelogenous leukemia AML with mutated NPM1. Am J Hemat. 2022;97(12):E462-E465.

23. Lachowiez CA, Asimomitis G, Bernard E, et al. Multimodal and data-driven assessment of myeloid neoplasms refines classification across disease states. Blood Cancer Discov. 2025;6(5):425-436.

24. Bill M, Eckardt J-N, Döhner K, et al. Differential prognostic impact of myelodysplasia-related gene mutations in a European cohort of 4978 intensively treated AML patients. Leukemia. 2026;40(1):63-71.

25. Heiblig M, Duployez N, Marceau A, et al. The impact of DNMT3A status on NPM1 MRD predictive value and survival in elderly AML patients treated intensively. Cancers (Basel). 2021;13(9):2156.

26. Sánchez AH, Ramiro AV, Sträng E, et al. Machine learning allows the identification of new co-mutational patterns with prognostic implications in NPM1 mutated AML - results of the european harmony alliance. Blood 2022;140(Supplement 1):739-742.

27. Levis M, Montesinos P, Kim H, et al. The combination of a FLT3-ITD, NPM1mut and an epigenetic regulatory gene mutation confers unique sensitivity to quizartinib: analysis from the Quantum-first trial. EHA Library. 2025;4159217:S140.

28. Su M, Fleischer T, Grosheva I, et al. Targeting SRSF2 mutations in leukemia with RKI-1447: A strategy to impair cellular division and nuclear structure. iScience. 2024;27(4):109443.

Tables

Table 1. Main characteristics of the entire cohort.

Feature	Total (n = 1,360)
Age (years)	**n (%)**
≤45	149 (10.96)
46-60	386 (28.38)
61-75	538 (39.56)
>75	287 (21.10)
Sex	
Male	643 (47.28)
Female	717 (52.72)
AML type	
de novo	928 (68.24)
Secondary	170 (12.50)
NA	262 (19.26)
ECOG	
0	424 (31.18)
1	363 (26.69)
2	115 (8.46)
3	42 (3.09)
4	15 (1.10)
NA	401 (29.48)
Cytogenetics	
Not Evaluable	76 (5.59)
Normal	712 (52.35)
Altered	218 (16.03)
NA	354 (26.03)
NPM1 type	
A	1,039 (76.40)
B	84 (6.18)
D	94 (6.91)
Non-ABD	143 (10.51)
Intensive treatment	
Yes	688 (50.59)
No	320 (23.53)
NA	352 (25.88)
Allogeneic transplantation	
Yes	163 (11.99)
No	773 (56.84)
NA	424 (31.18)
WBC, median (range)	24.95 (0.13-483.24)
Hemoglobin, median (range)	8.89 (1.89-15.9)
Platelet, median (range)	62.5 (0.90-939)
Bone marrow blasts, median (range)	72 (1-100)

LDH, median (range)	482 (1-13190)

WBC: white blood cell count; LDH: lactate dehydrogenase; NA: Not available.

Table 2. Multivariable Cox regression model including clinical covariates and selected genetic variables in the intensive therapy cohort.

	Overall Survival (OS)				**Relapse-Free Survival (RFS)**				**Event-Free Survival (EFS)**			
Feature	**HR**	**95 % CI low**	**95% CI high**	**p.value**	**HR**	**95% CI low**	**95% CI high**	**p.value**	**HR**	**95 % CI low**	**95% CI high**	**p.value**
Age (continous)	1.04	1.02	1.05	**<0.001**	1.03	1.01	1.04	**<0.001**	1.03	1.01	1.04	**<0.001**
Sex: Female vs Male	0.95	0.70	1.28	0.725	0.98	0.75	1.29	0.891	0.99	0.75	1.29	0.923
AML type: secondary vs de novo	1.07	0.68	1.66	0.779	1.08	0.73	1.62	0.693	1.13	0.77	1.68	0.530
Cytogenetics: Altered vs Normal	1.22	0.82	1.81	0.324	1.19	0.83	1.70	0.357	1.16	0.82	1.66	0.402
MR-genes count: 1 vs 0	0.72	0.38	1.37	0.317	0.70	0.40	1.24	0.223	0.69	0.39	1.20	0.188
MR-genes count: ≥2 vs 0	1.09	0.40	2.98	0.868	0.72	0.26	1.98	0.523	0.65	0.23	1.81	0.410
ETV6 (mut)	1.95	0.72	5.31	0.190	1.66	0.66	4.20	0.281	1.52	0.61	3.83	0.371
FLT3-ITD (mut)	1.49	0.90	2.03	0.104	1.19	0.90	1.57	0.227	1.22	0.92	1.60	0.162
FLT3-OTHER (mut)	0.60	0.32	0.91	**0.010**	0.61	0.36	1.02	0.057	0.64	0.39	1.05	0.077
SRSF2 (mut)	1.98	1.15	4.12	**0.037**	2.74	1.43	5.28	**0.002**	2.74	1.43	5.24	**0.002**
KRAS (mut)	1.96	1.21	3.17	**0.006**	1.50	0.95	2.36	0.079	1.55	0.99	2.41	0.054
NRAS (mut)	0.78	0.48	1.26	0.314	0.81	0.53	1.23	0.321	0.77	0.51	1.16	0.215
DNMT3A (mut)	1.22	0.90	1.66	0.202	1.53	1.16	2.03	**0.003**	1.47	1.12	1.94	**0.006**
PTPN11 (mut)	0.85	0.51	1.43	0.548	0.68	0.43	1.09	0.107	0.72	0.46	1.14	0.159

Figures

Figure 1. Genomic landscape and co-mutation structure in *NPM1*-mutated AML. (A) Oncoprint of 1,360 adults showing per-gene mutation frequencies (right bars) and per-patient mutation calls (columns). Top tracks indicate total mutation burden per case; bottom annotations display age group, upfront intensive treatment, sex, AML type, and reference laboratory.

Figure 2. Age and genomic distribution by *NPM1* type. (A) Distribution of NPM1 mutation types across age groups. (B) Frequency of co-mutations according to *NPM1* type. (C) Heatmap depicting the proportion of mutated genes across *NPM1* types, with standardized residuals indicating over-representation (●) or under-representation (×).

Figure 3. Phenotypic associations and outcome impact of co-mutations in *NPM1*-mutated AML. (A) Bubble plots showing associations between specific co-mutated doublets and baseline clinical features. The x-axis represents effect size relative to other patients, the y-axis shows statistical significance (–log10 *P*), and bubble size reflects the number of patients carrying each co-mutation. (B) Forest plots summarizing the effect of multiple mutations within individual genes or functional pathways. Each dot represents the estimated effect size relative to single-mutant cases, with horizontal lines indicating 95% confidence intervals. Colors denote false-discovery–adjusted significance thresholds ($q<0.1$, $q<0.3$, or >0.3).

Figure 4. Impact of MR-gene mutations in the intensively treated *NPM1*-mutated AML (n=688). (A) Proportion of patients harboring MR-gene mutations and distribution of individual MR-genes among positive cases, patients harboring more than one MR-gene mutation contribute to each relevant gene category, and the plot does not distinguish between single and multiple MR-gene mutations. (B) OS of patients with ≥2 MR-gene mutations compared with those with none or one MR-gene mutation.

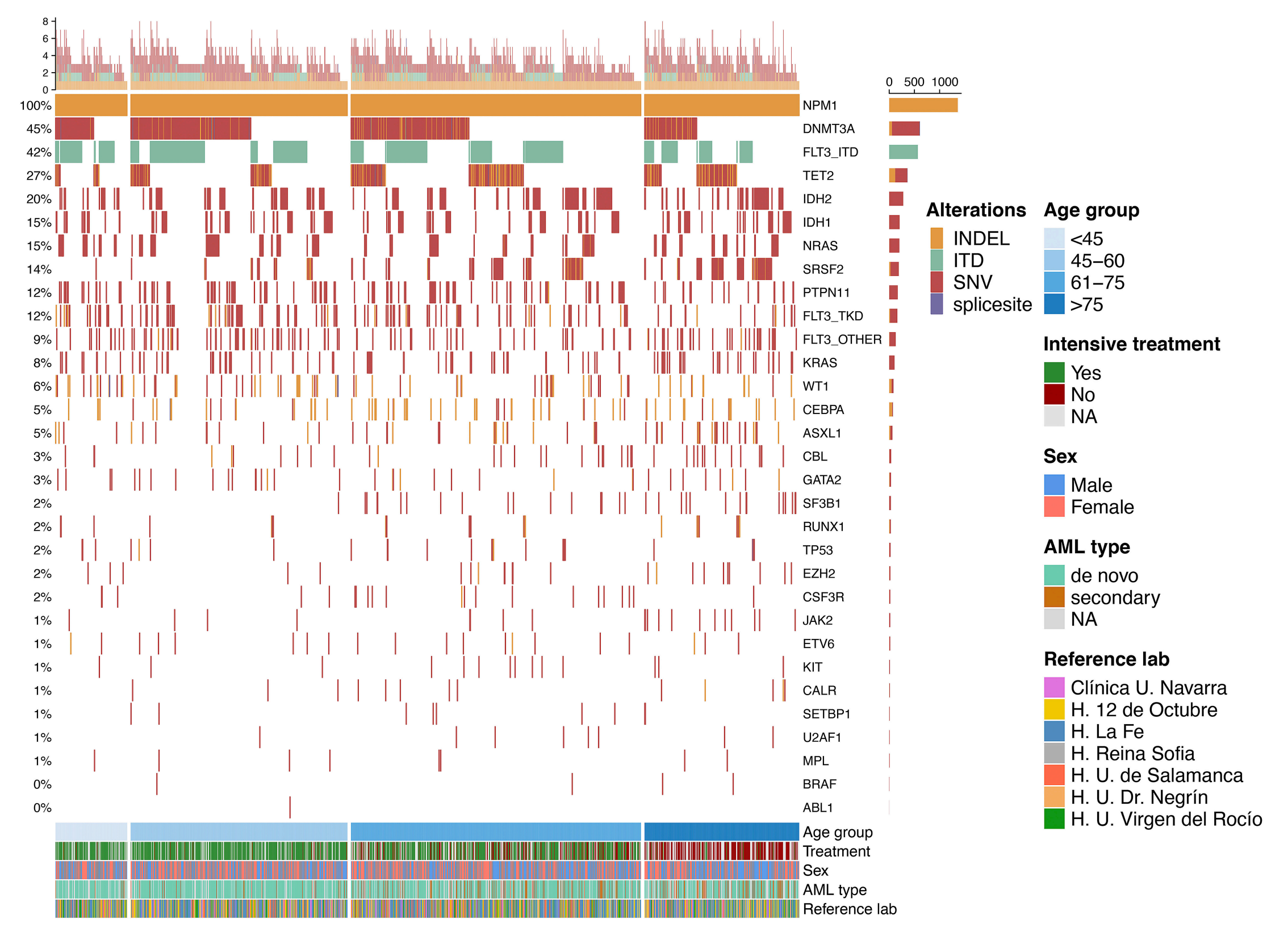
8
6
4
2
0
0 500 1000
100% NPM1
45% DNMT3A
42% FLT3_ITD
27% TET2
20% IDH2
15% IDH1
15% NRAS
14% SRSF2
12% PTPN11
12% FLT3_TKD
9% FLT3_OTHER
8% KRAS
6% WT1
5% CEBPA
5% ASXL1
3% CBL
3% GATA2
2% SF3B1
2% RUNX1
2% TP53
2% EZH2
2% CSF3R
1% JAK2
1% ETV6
1% KIT
1% CALR
1% SETBP1
1% U2AF1
1% MPL
0% BRAF
0% ABL1
Age group
Treatment
Sex
AML type
Reference lab
Alterations
INDEL
ITD
SNV
splicesite
Age group
<45
45–60
61–75
>75
Intensive treatment
Yes
No
NA
Sex
Male
Female
AML type
de novo
secondary
NA
Reference lab
Clínica U. Navarra
H. 12 de Octubre
H. La Fe
H. Reina Sofia
H. U. de Salamanca
H. U. Dr. Negrín
H. U. Virgen del Rocío

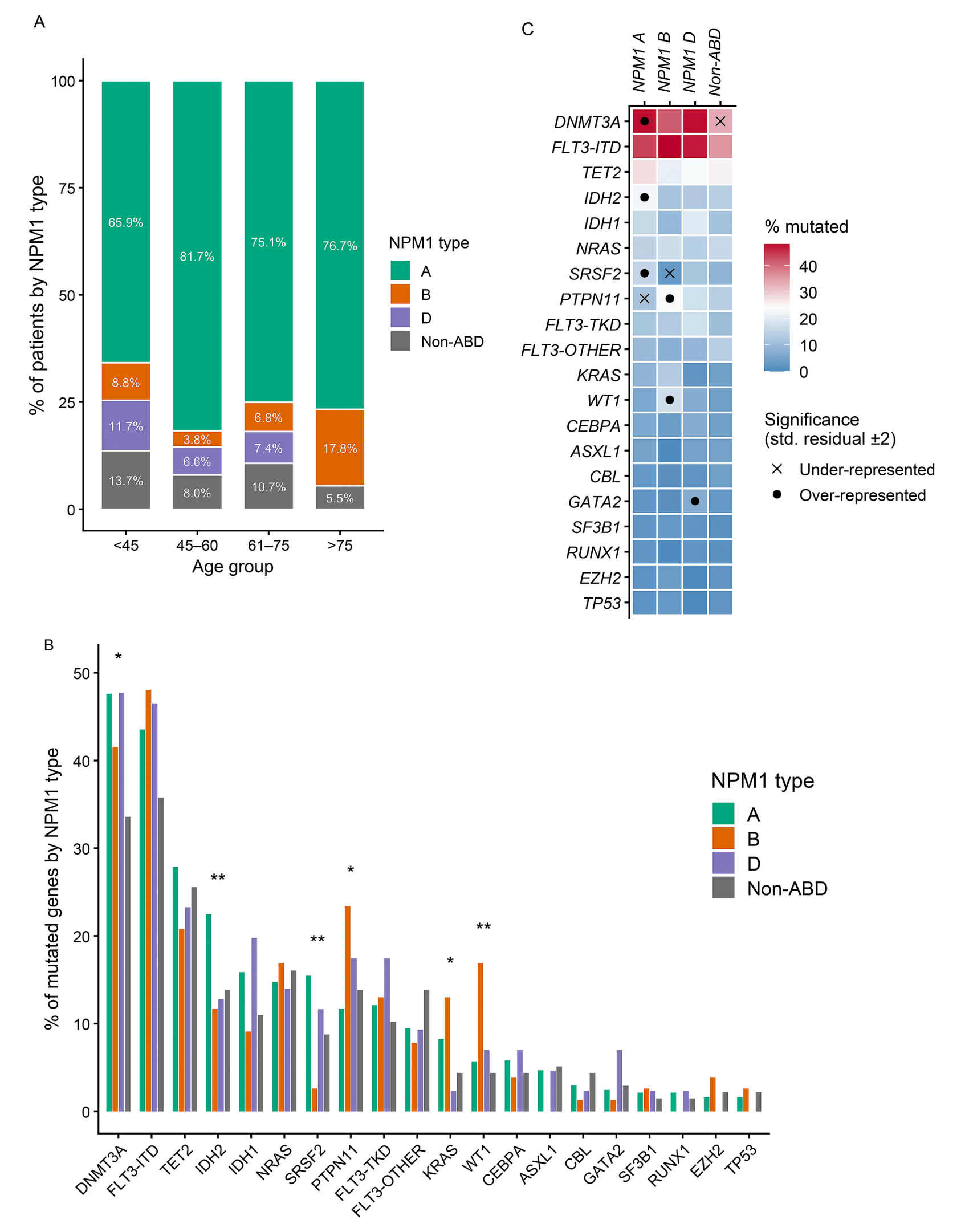
A
% of patients by NPM1 type
100
75
50
25
0
65.9%
8.8%
11.7%
13.7%
81.7%
3.8%
6.6%
8.0%
75.1%
6.8%
7.4%
10.7%
76.7%
17.8%
5.5%
<45
45–60
61–75
>75
Age group
NPM1 type
A
B
D
Non-ABD
C
NPM1 A
NPM1 B
NPM1 D
Non-ABD
DNMT3A
FLT3-ITD
TET2
IDH2
IDH1
NRAS
SRSF2
PTPN11
FLT3-TKD
FLT3-OTHER
KRAS
WT1
CEBPA
ASXL1
CBL
GATA2
SF3B1
RUNX1
EZH2
TP53
% mutated
40
30
20
10
0
Significance
(std. residual ±2)
Under-represented
Over-represented
B
% of mutated genes by NPM1 type
50
40
30
20
10
0
*
**
**
*
*
**
DNMT3A
FLT3-ITD
TET2
IDH2
IDH1
NRAS
SRSF2
PTPN11
FLT3-TKD
FLT3-OTHER
KRAS
WT1
CEBPA
ASXL1
CBL
GATA2
SF3B1
RUNX1
EZH2
TP53
NPM1 type
A
B
D
Non-ABD

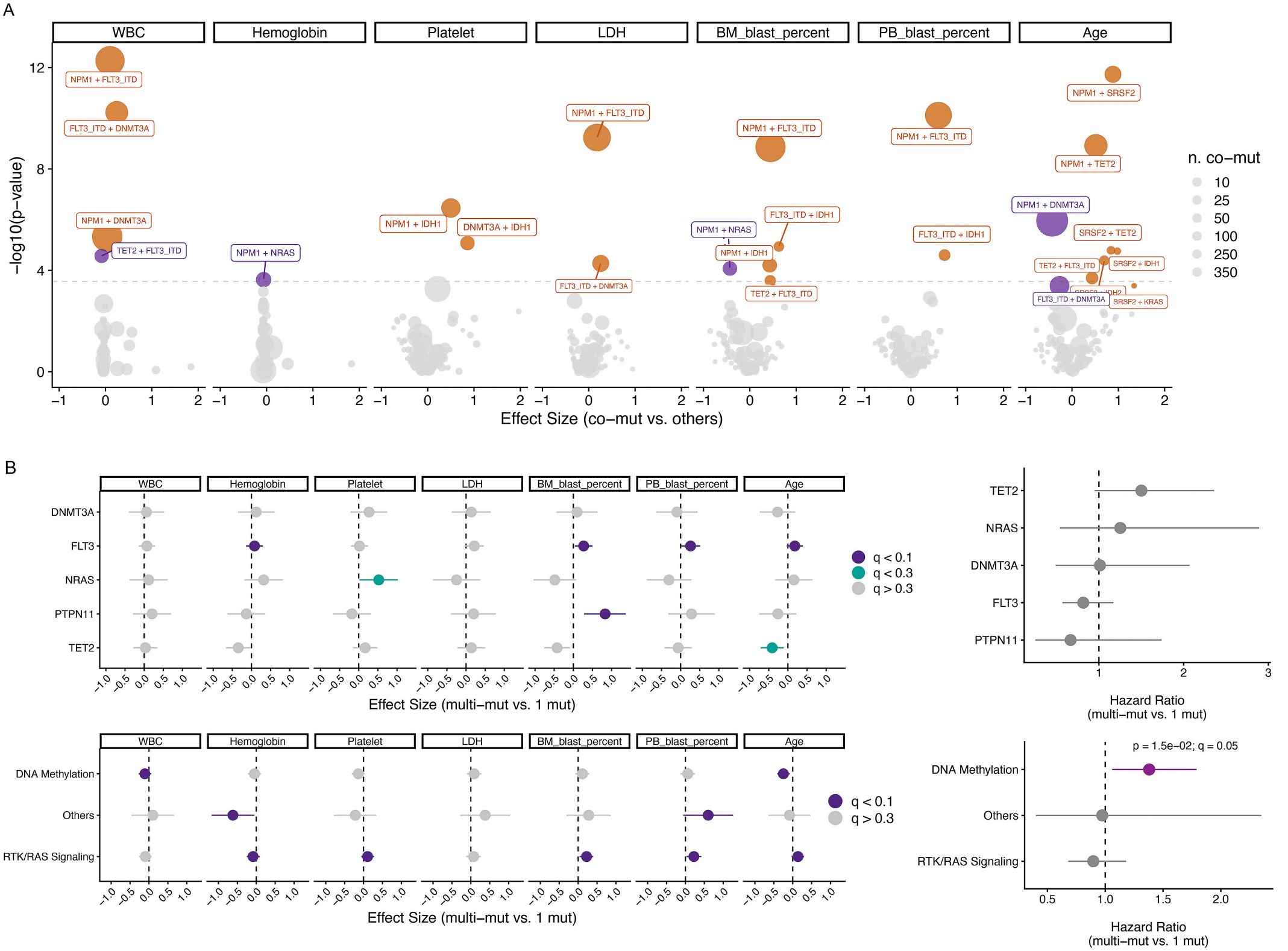
A
WBC
Hemoglobin
Platelet
LDH
BM_blast_percent
PB_blast_percent
Age
−log10(p−value)
Effect Size (co−mut vs. others)
n. co−mut
10
25
50
100
250
350
NPM1 + FLT3_ITD
FLT3_ITD + DNMT3A
NPM1 + DNMT3A
TET2 + FLT3_ITD
NPM1 + NRAS
NPM1 + IDH1
DNMT3A + IDH1
FLT3_ITD + IDH1
NPM1 + SRSF2
NPM1 + TET2
SRSF2 + TET2
SRSF2 + IDH1
SRSF2 + KRAS
B
DNMT3A
FLT3
NRAS
PTPN11
TET2
Effect Size (multi−mut vs. 1 mut)
q < 0.1
q < 0.3
q > 0.3
Hazard Ratio
(multi−mut vs. 1 mut)
DNA Methylation
Others
RTK/RAS Signaling
p = 1.5e−02; q = 0.05

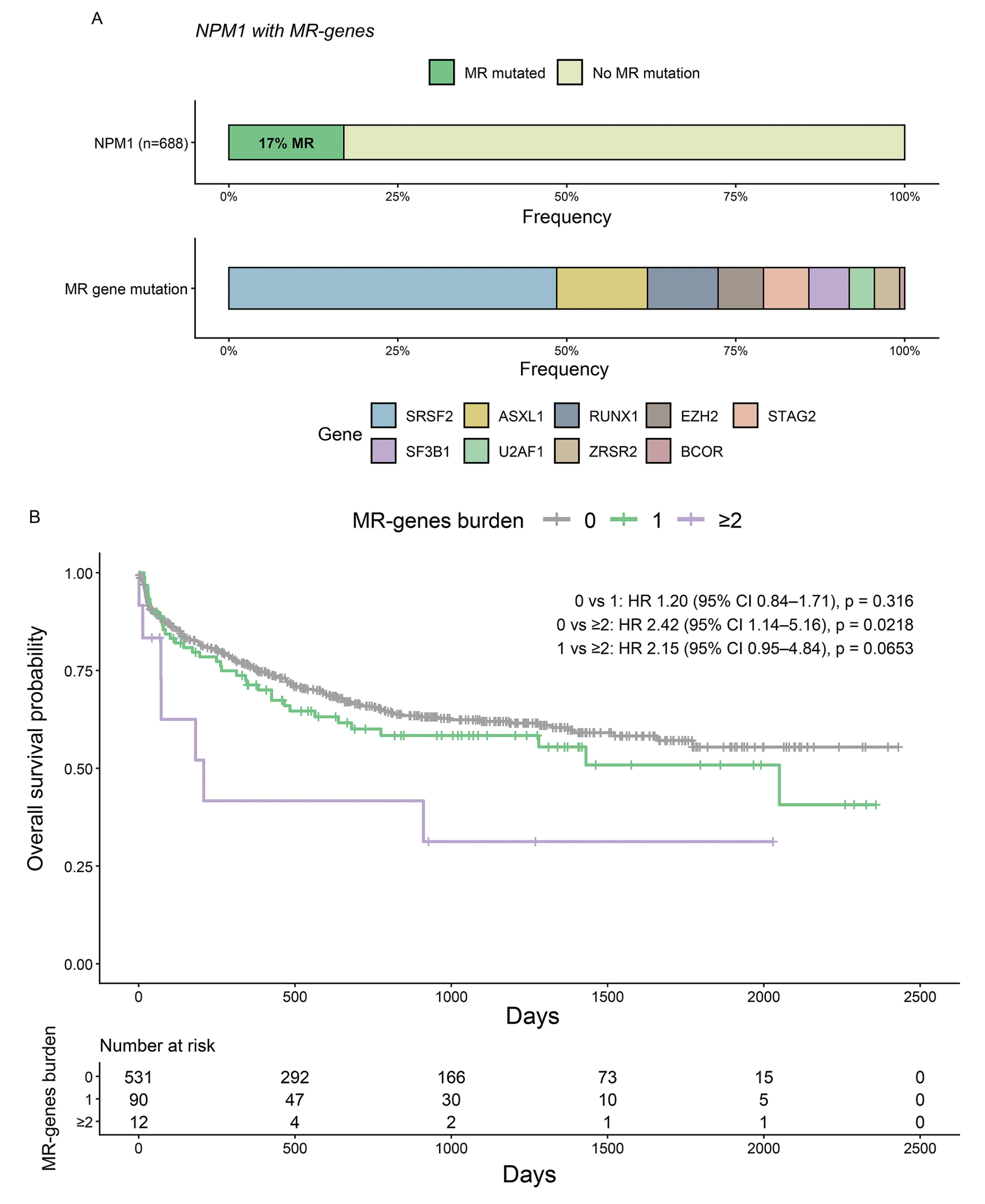
A
NPM1 with MR-genes
MR mutated
No MR mutation
NPM1 (n=688)
17% MR
0%
25%
50%
75%
100%
Frequency
MR gene mutation
0%
25%
50%
75%
100%
Frequency
Gene
SRSF2
ASXL1
RUNX1
EZH2
STAG2
SF3B1
U2AF1
ZRSR2
BCOR
B
MR-genes burden
0
1
≥2
0 vs 1: HR 1.20 (95% CI 0.84–1.71), p = 0.316
0 vs ≥2: HR 2.42 (95% CI 1.14–5.16), p = 0.0218
1 vs ≥2: HR 2.15 (95% CI 0.95–4.84), p = 0.0653
Overall survival probability
1.00
0.75
0.50
0.25
0.00
0
500
1000
1500
2000
2500
Days
Number at risk
MR-genes burden
0 531 292 166 73 15 0
1 90 47 30 10 5 0
≥2 12 4 2 1 1 0
0
500
1000
1500
2000
2500
Days

Supplemental Figures

Supplemental Figure 1. Distribution of mutation counts per patient. Histogram showing the number of co-mutations per patient in the *NPM1*-mutated AML cohort (n=1,360). Bars represent the absolute number of patients for each mutation count, with percentages indicated above.

Supplemental Figure 2. Gene-level clonal evolution from diagnosis to relapse in paired NPM1-mutated AML samples. (A) Heatmap showing the distribution of stable, lost, and gained mutations across recurrently mutated genes in paired diagnostic and relapse samples. (B) Stacked bar plot summarizing the proportion of stable, lost, and gained events for each gene.

Supplemental Figure 3. Age-resolved distribution of co-mutations in *NPM1*-mutated AML. (A) Number of patients stratified into four age groups (≤45, 46–60, 61–75, >75 years). (B) Per-gene prevalence across age groups. (C) Pathway-level summaries across age groups.

Supplemental Figure 4. Continuous age trends and age-specific association architecture. (A) Generalized additive models (logit) depicting continuous age–prevalence trajectories for significantly age-variant genes. (B) Dot plot representing age-dependent shifts. Each point's size and fill encode within-group prevalence (percentage of patients with ≥1 mutation in that gene). Shapes indicate pairwise differences across age groups using Fisher's exact tests with Benjamini–Hochberg correction within each gene. (C) Age-stratified circos diagrams displaying the structure of co-mutation networks within each age category; line thickness is proportional to the strength of co-occurrence. (D) Heatmaps of pairwise associations showing co-occurrence (red) and mutual exclusivity (blue) between genes across age strata; color intensity reflects odds ratios and significance levels.

Supplemental Figure 5. Gene-wise prevalence and age-stratified odds ratios in *NPM1*-mutated AML. For each gene, the left panel shows prevalence within each age group (≤45, 46–60, 61–75, >75 years) with Wilson 95% confidence intervals. The right panel shows odds ratios (ORs) and 95% CIs comparing each age group to the reference group (≤45 years). Asterisks indicate BH-adjusted significance levels (**p*<0.05, ***p*<0.01, ****p*<0.001).

Supplemental Figure 6. Overall survival by *NPM1* mutation type in intensively treated patients. Kaplan–Meier curves comparing OS among *NPM1* mutation types (A, B, D, and Non-ABD) in the cohort of 688 patients who received up-front intensive therapy.

Supplemental Figure 7. Forest plot of univariate Cox regression models showing hazard ratios (HRs) for overall survival by individual gene mutations. Each bar represents the 95% confidence interval; vertical dashed line indicates HR=1. Genes are grouped by functional class and color-coded accordingly.

Supplemental Figure 8. Survival and cumulative incidence of relapse according to MRD status in *NPM1*-mutated AML. (A) OS according to post-induction MRD status in the subset of patients with available MRD data. Kaplan-Meier curves are shown with the corresponding log-rank p-value. (B) CIR according to post-induction MRD status. Gray's test p-value is indicated.

Supplemental Figure 9. Overall survival according to FLT3-inhibitor use in intensively treated patients with *NPM1*-mutated and *FLT3*-ITD–positive AML. Kaplan–Meier curves comparing patients treated with FLT3 inhibitors (FLT3i; green) versus those who did not receive FLT3i (red).

Supplemental Figure 10. Kaplan–Meier curves for overall survival by gene mutation status in intensively treated *NPM1*-mutated AML. Each panel shows overall survival for patients carrying the indicated gene mutation (red) compared with wild-type cases (gray). Log-rank *p* values and hazard ratios (HR, with 95% CI) are displayed within each plot.

Supplemental Figure 11. Survival outcomes according to *FLT3*-ITD microclone status in intensively treated *NPM1*-mutated AML. (A) OS, (B) RFS, and (C) EFS stratified as no *FLT3*-ITD, *FLT3* microclone, and *FLT3*-ITD ≥0.05. Kaplan-Meier curves include log-rank p-values, pairwise HRs with 95% CIs, and median survival estimates.

Supplemental Figure 12. OS of patients carrying a single MR-gene mutation compared with MR-negative cases. *BCOR* was excluded due to its low frequency.

Supplemental Figure 13. Prognostic impact of triple-mutated genotypes in *NPM1*-mutated AML. (A) Bar plot showing the frequency of three-gene constellations observed in at least 10 patients. Bars are annotated with the number of patients; those highlighted in red indicate triads with a significant association

with survival. (B) Forest plot of hazard ratios for overall survival comparing patients with specific triads versus the corresponding pairwise background. Dot size reflects the number of patients with each triad, and horizontal lines indicate 95% confidence intervals. Representative Kaplan–Meier survival curves for selected triads are shown on the right, with survival estimates compared between patients carrying the triad, the corresponding doublet, and all others.

Supplemental Figure 14. Overall survival in patients with the *NPM1:DNMT3A:FLT3*-ITD triad stratified by *DNMT3A* hotspot status and FLT3-inhibitor use. (A) Kaplan–Meier curves comparing OS among patients with *NPM1:DNMT3A:FLT3*-ITD, separated into *DNMT3A* R882 and non-R882 carriers, and contrasted with the remainder of the cohort. (B) OS of patients with the *NPM1:DNMT3A:FLT3*-ITD triad according to FLT3-inhibitor treatment (FLT3i vs no FLT3i). HRs, 95% CI, and p values are displayed on the plot.

Online Supplementary Tables 1-15 provided as Excel file only.

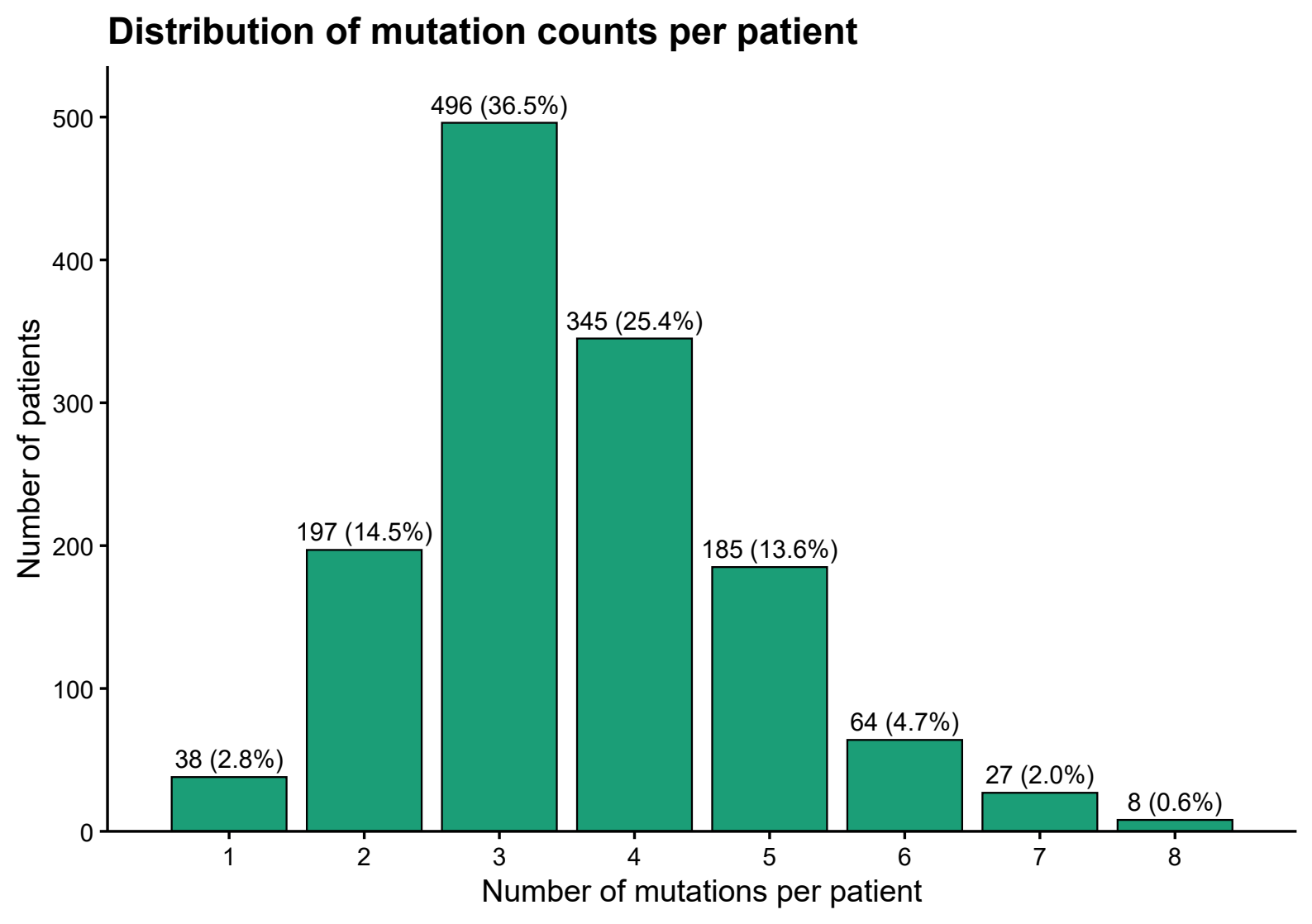
Distribution of mutation counts per patient
Number of patients
Number of mutations per patient
0
100
200
300
400
500
1
2
3
4
5
6
7
8
38 (2.8%)
197 (14.5%)
496 (36.5%)
345 (25.4%)
185 (13.6%)
64 (4.7%)
27 (2.0%)
8 (0.6%)

A

Gene-level clonal evolution from diagnosis to relapse

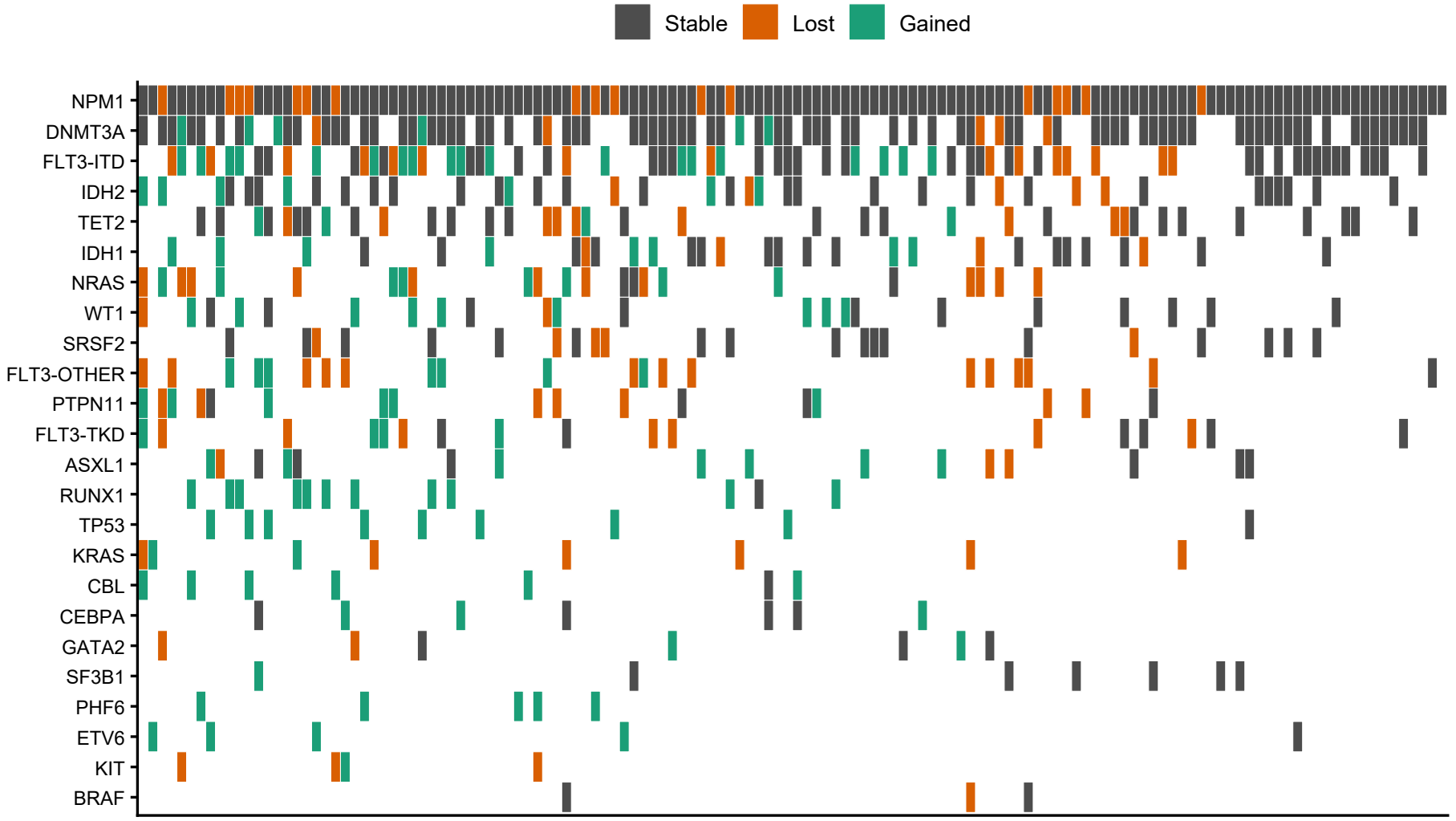

B

Gene-level stability, loss and gain at relapse

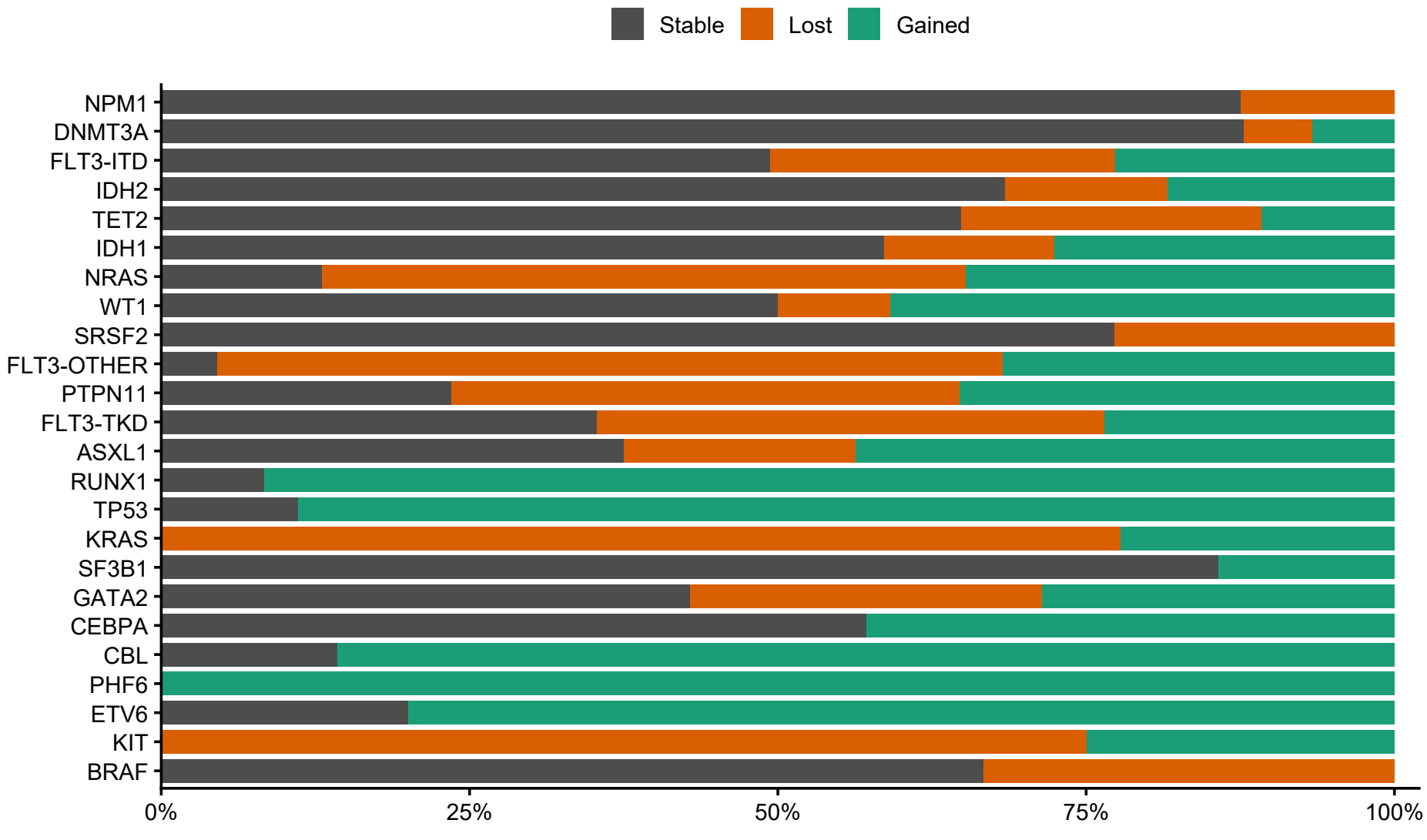

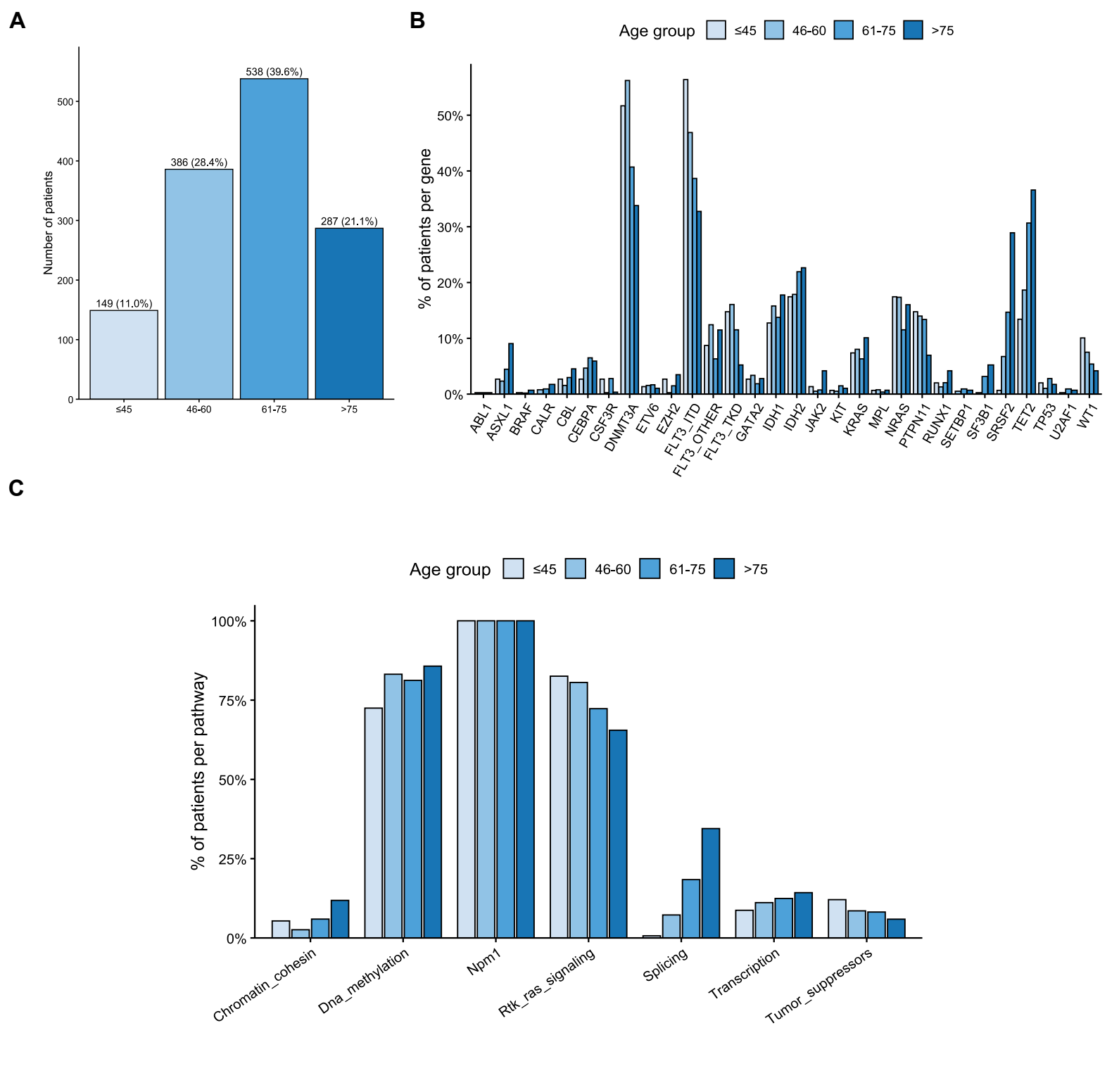
A
Number of patients
538 (39.6%)
386 (28.4%)
287 (21.1%)
149 (11.0%)
≤45
46-60
61-75
>75
B
Age group
≤45
46-60
61-75
>75
% of patients per gene
ABL1
ASXL1
BRAF
CALR
CBL
CEBPA
CSF3R
DNMT3A
ETV6
EZH2
FLT3_ITD
FLT3_OTHER
FLT3_TKD
GATA2
IDH1
IDH2
JAK2
KIT
KRAS
MPL
NRAS
PTPN11
RUNX1
SETBP1
SF3B1
SRSF2
TET2
TP53
U2AF1
WT1
C
Age group
≤45
46-60
61-75
>75
% of patients per pathway
Chromatin_cohesin
Dna_methylation
Npm1
Rtk_ras_signaling
Splicing
Transcription
Tumor_suppressors

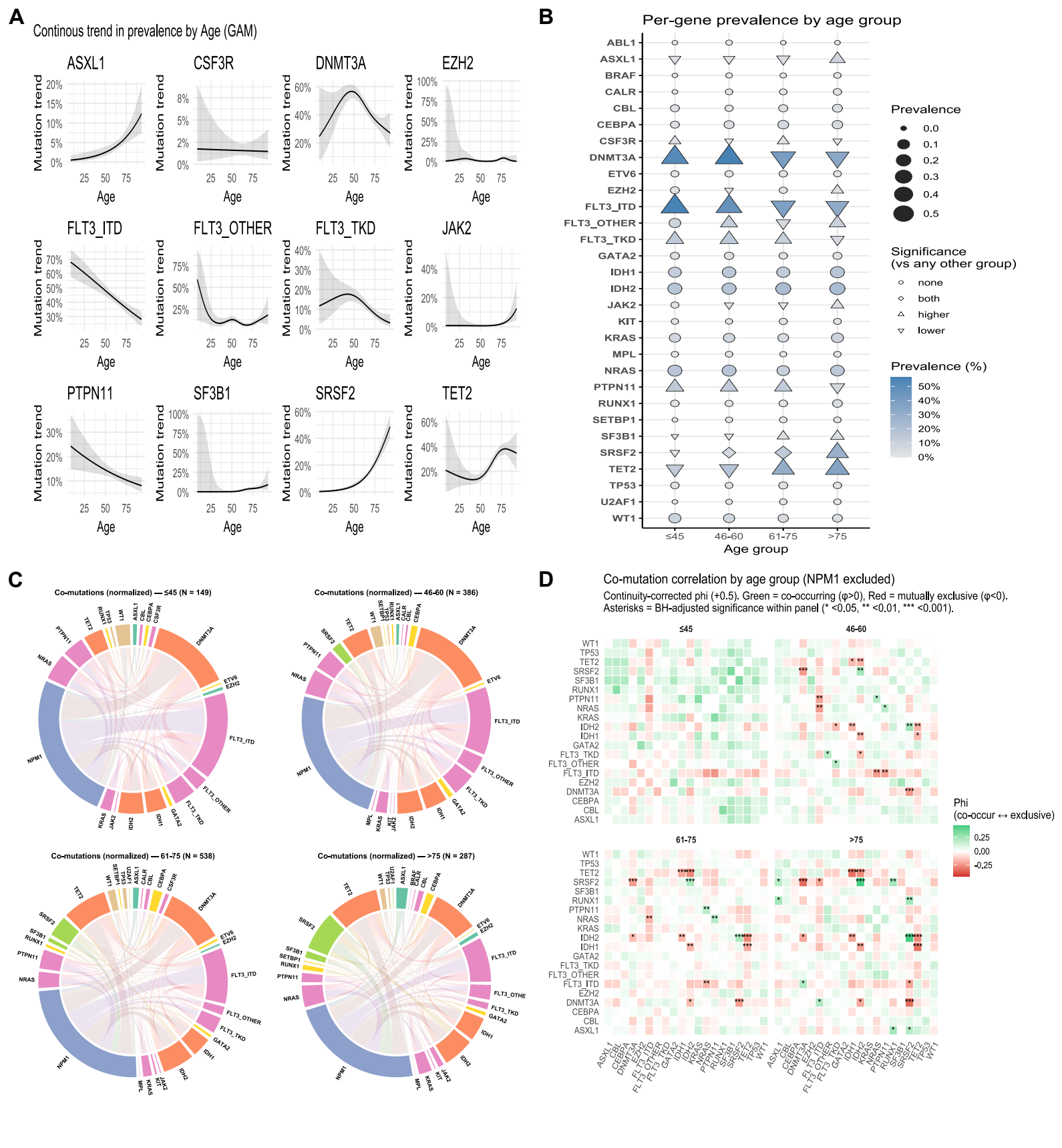
A
Continous trend in prevalence by Age (GAM)
ASXL1
CSF3R
DNMT3A
EZH2
FLT3_ITD
FLT3_OTHER
FLT3_TKD
JAK2
PTPN11
SF3B1
SRSF2
TET2
Mutation trend
Age
B
Per-gene prevalence by age group
ABL1
ASXL1
BRAF
CALR
CBL
CEBPA
CSF3R
DNMT3A
ETV6
EZH2
FLT3_ITD
FLT3_OTHER
FLT3_TKD
GATA2
IDH1
IDH2
JAK2
KIT
KRAS
MPL
NRAS
PTPN11
RUNX1
SETBP1
SF3B1
SRSF2
TET2
TP53
U2AF1
WT1
≤45
46-60
61-75
>75
Age group
Prevalence
0.0
0.1
0.2
0.3
0.4
0.5
Significance
(vs any other group)
none
both
higher
lower
Prevalence (%)
50%
40%
30%
20%
10%
0%
C
Co-mutations (normalized) — ≤45 (N = 149)
Co-mutations (normalized) — 46-60 (N = 386)
Co-mutations (normalized) — 61-75 (N = 538)
Co-mutations (normalized) — >75 (N = 287)
D
Co-mutation correlation by age group (NPM1 excluded)
Continuity-corrected phi (+0.5). Green = co-occurring (φ>0), Red = mutually exclusive (φ<0).
Asterisks = BH-adjusted significance within panel (* <0.05, ** <0.01, *** <0.001).
≤45
46-60
61-75
>75
Phi
(co-occur ↔ exclusive)
0.25
0.00
-0.25

Gene-wise prevalence and OR by age group (NPM1+ cohort)

Left: prevalence per age group (Wilson 95% CI). Right: odds ratio vs reference group ≤45 (Fisher/Wald CI). Stars denote BH-adjusted p-values within gene (*** <0.001, ** <0.01, * <0.05).

ASXL1

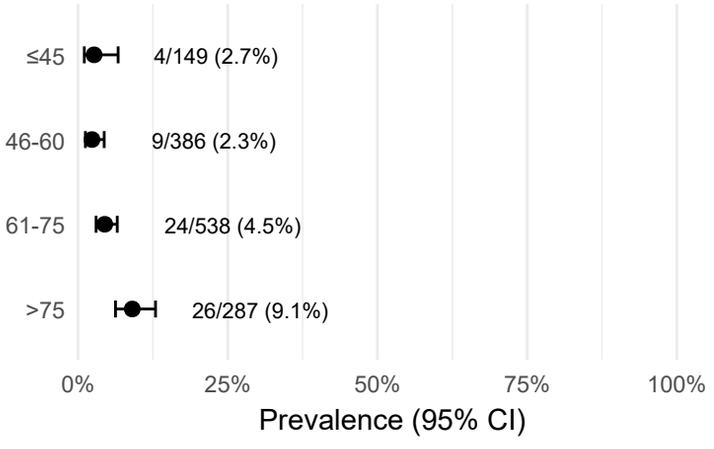

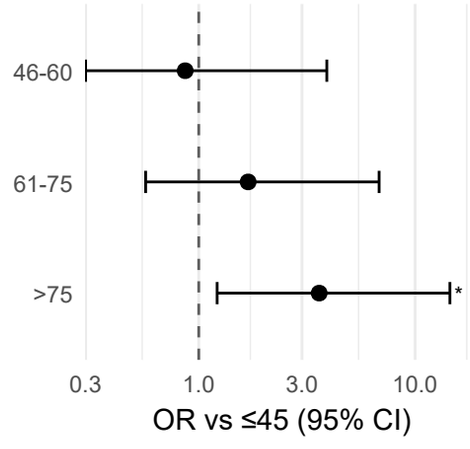

CSF3R

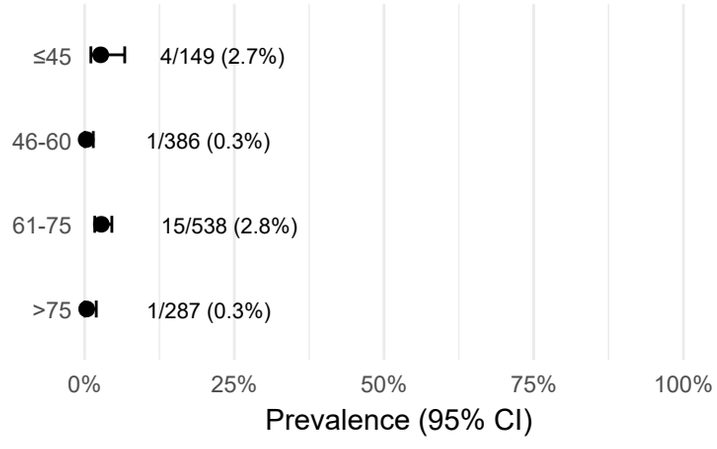

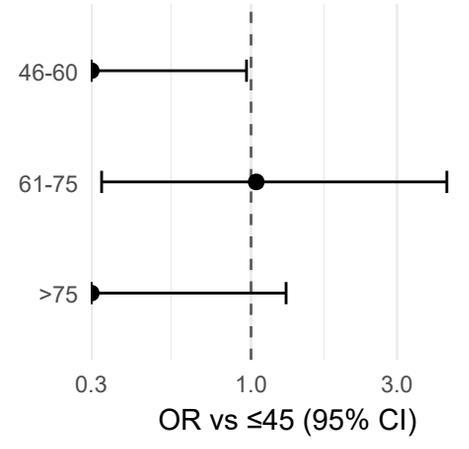

DNMT3A

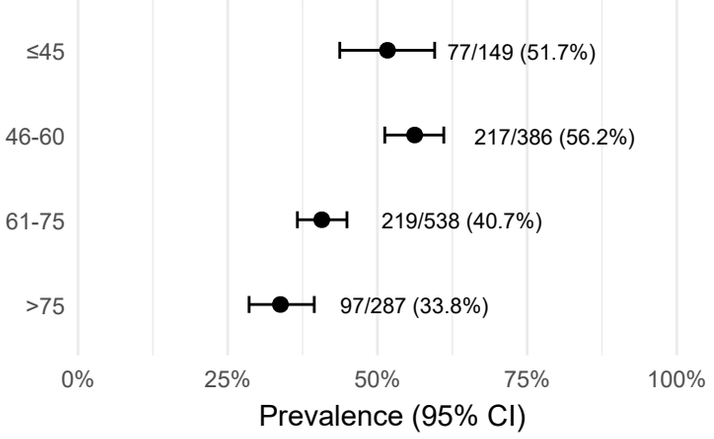

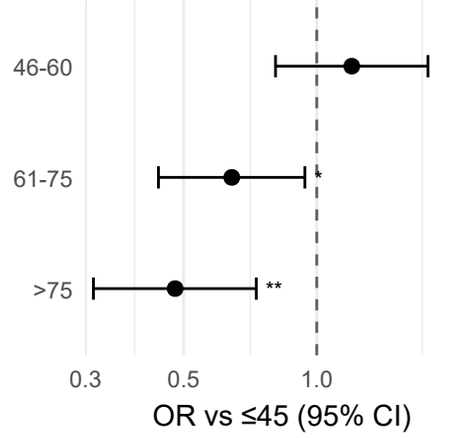

EZH2

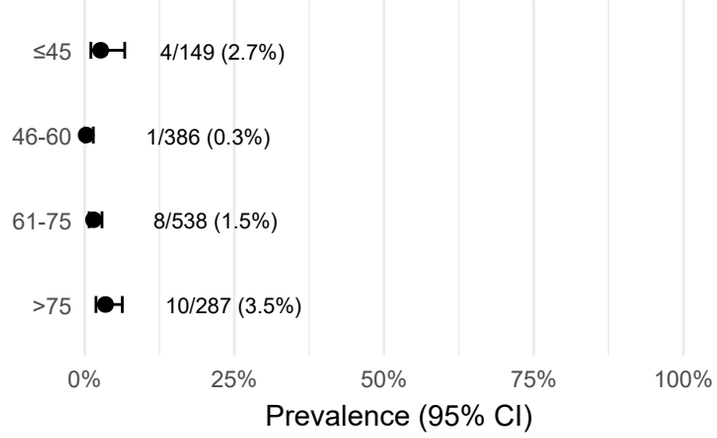

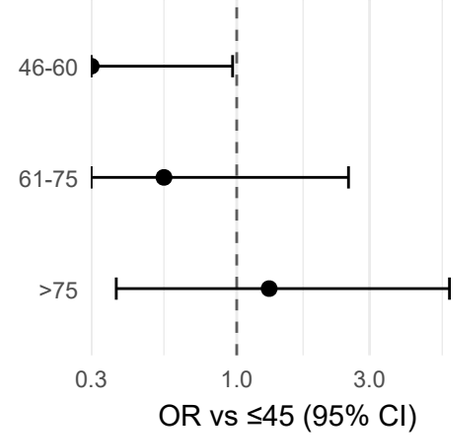

FLT3_ITD

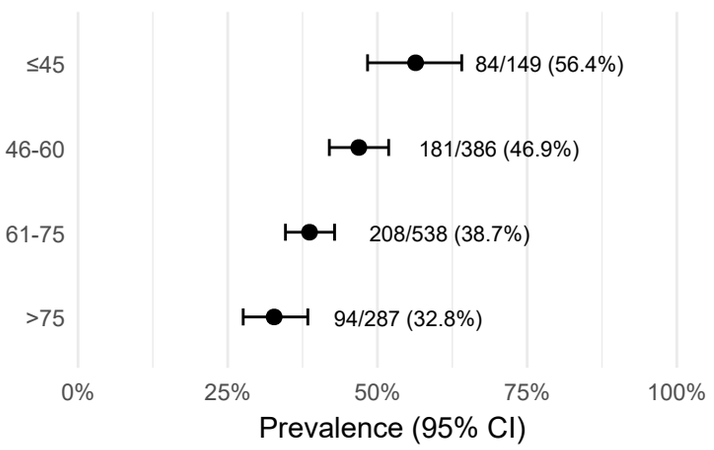

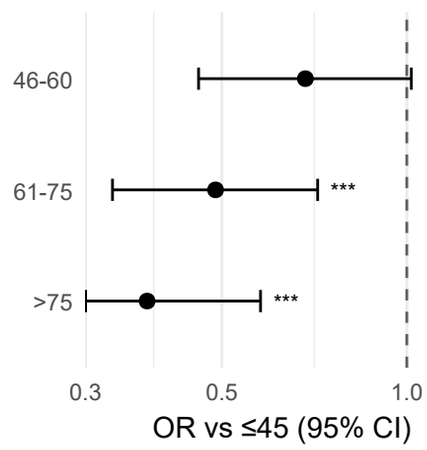

FLT3_OTHER

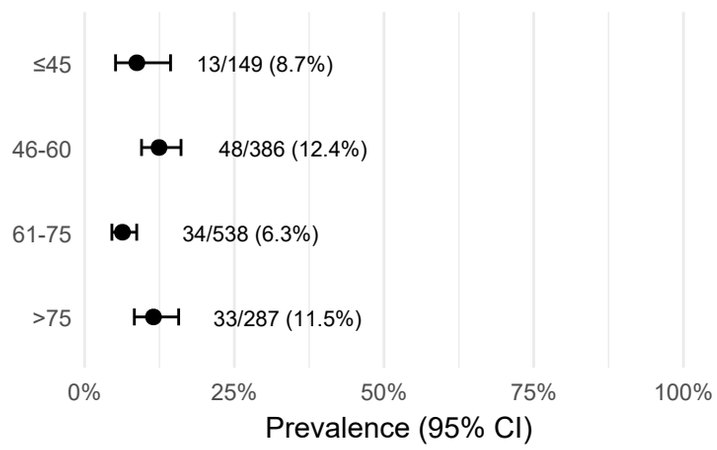

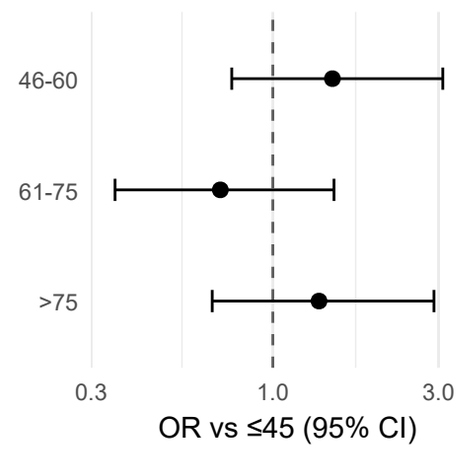

FLT3_TKD

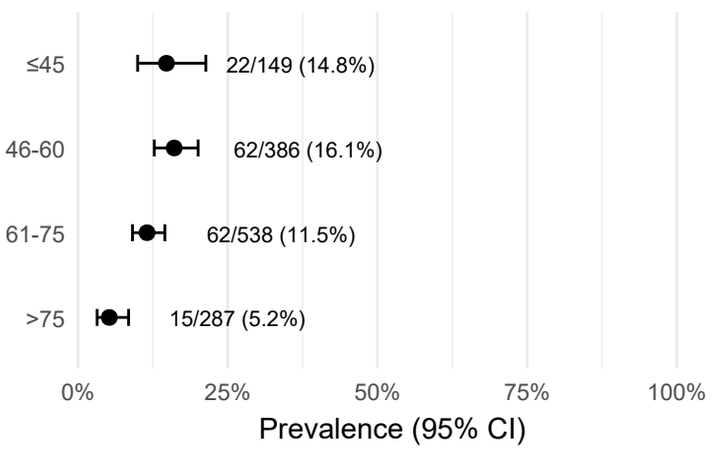

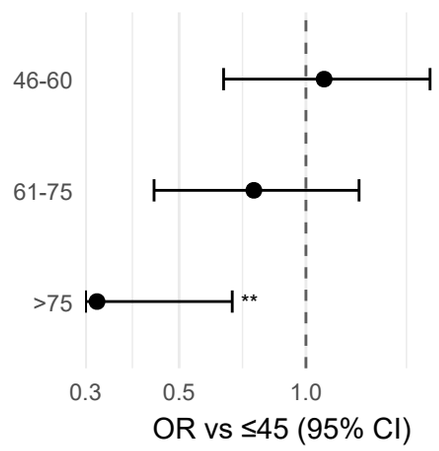

JAK2

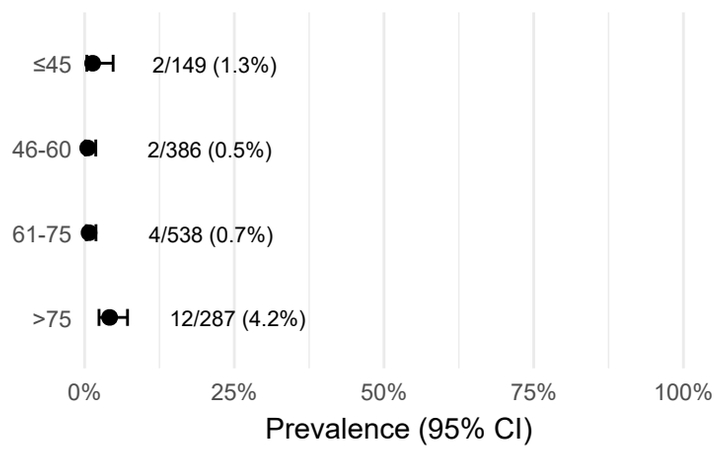

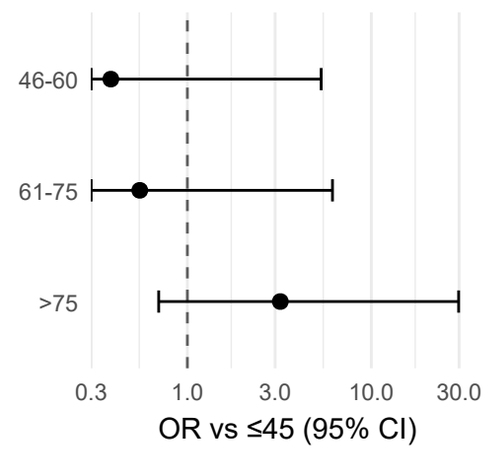

PTPN11

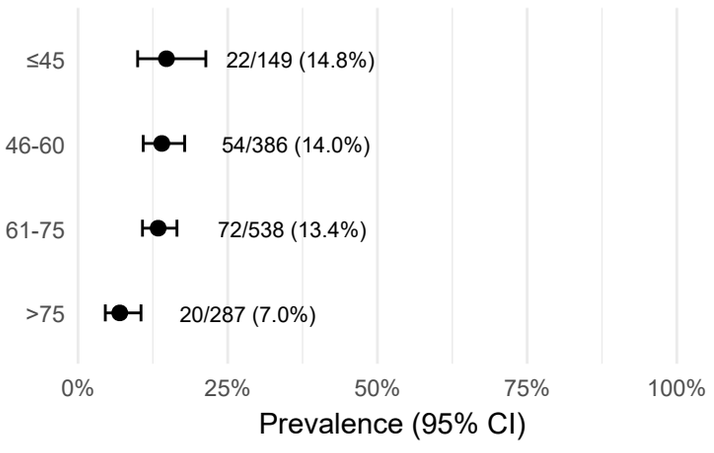

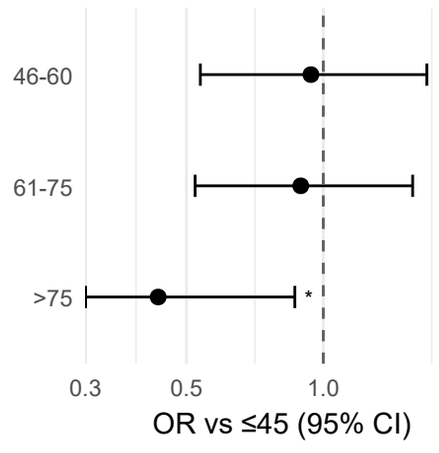

SF3B1

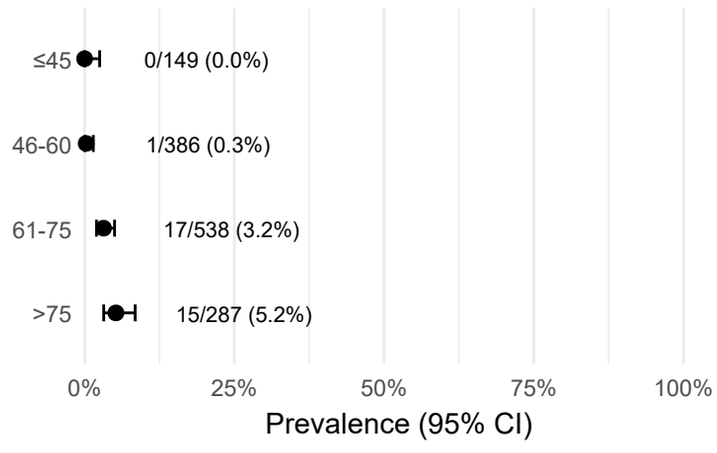

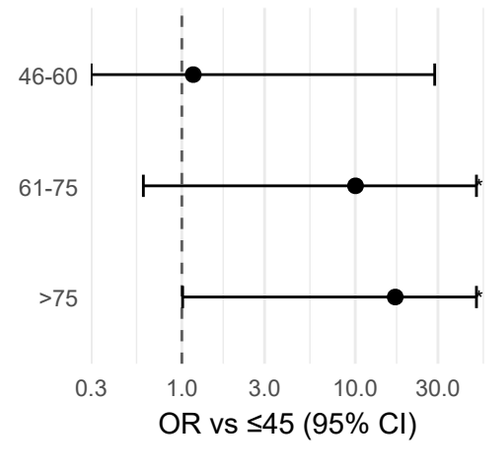

SRSF2

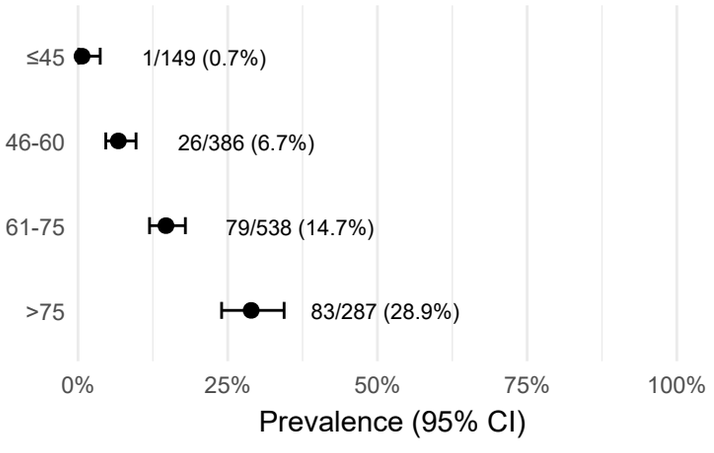

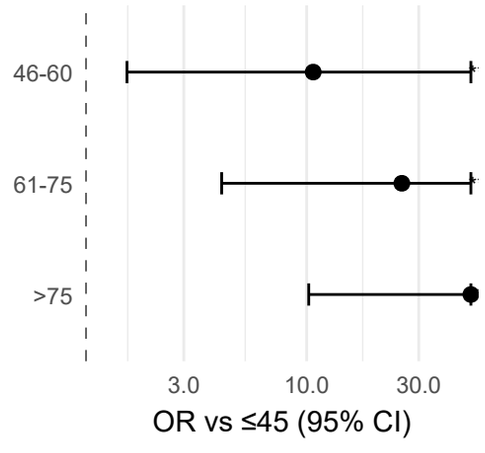

TET2

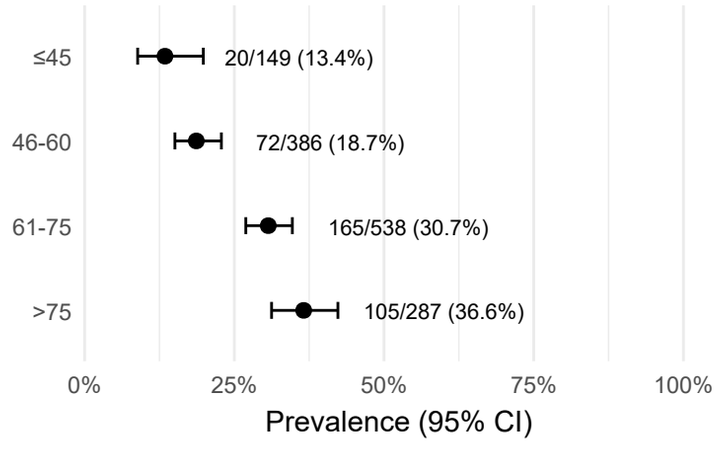

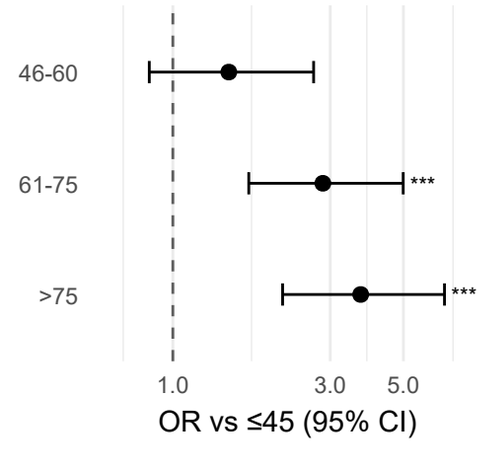

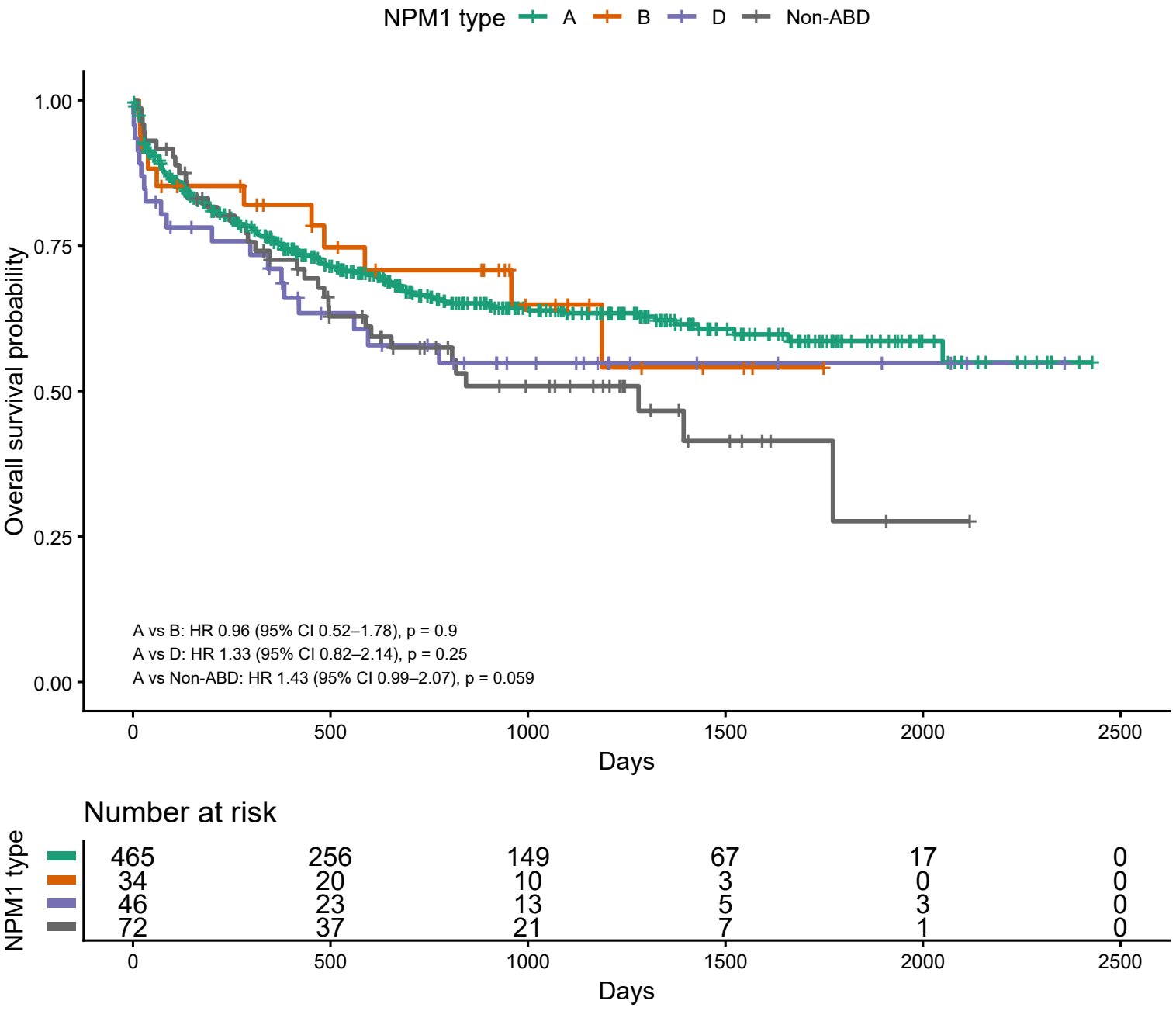
NPM1 type
A
B
D
Non-ABD
Overall survival probability
1.00
0.75
0.50
0.25
0.00
A vs B: HR 0.96 (95% CI 0.52–1.78), p = 0.9
A vs D: HR 1.33 (95% CI 0.82–2.14), p = 0.25
A vs Non-ABD: HR 1.43 (95% CI 0.99–2.07), p = 0.059
0
500
1000
1500
2000
2500
Days
Number at risk
NPM1 type
465 256 149 67 17 0
34 20 10 3 0 0
46 23 13 5 3 0
72 37 21 7 1 0
0
500
1000
1500
2000
2500
Days

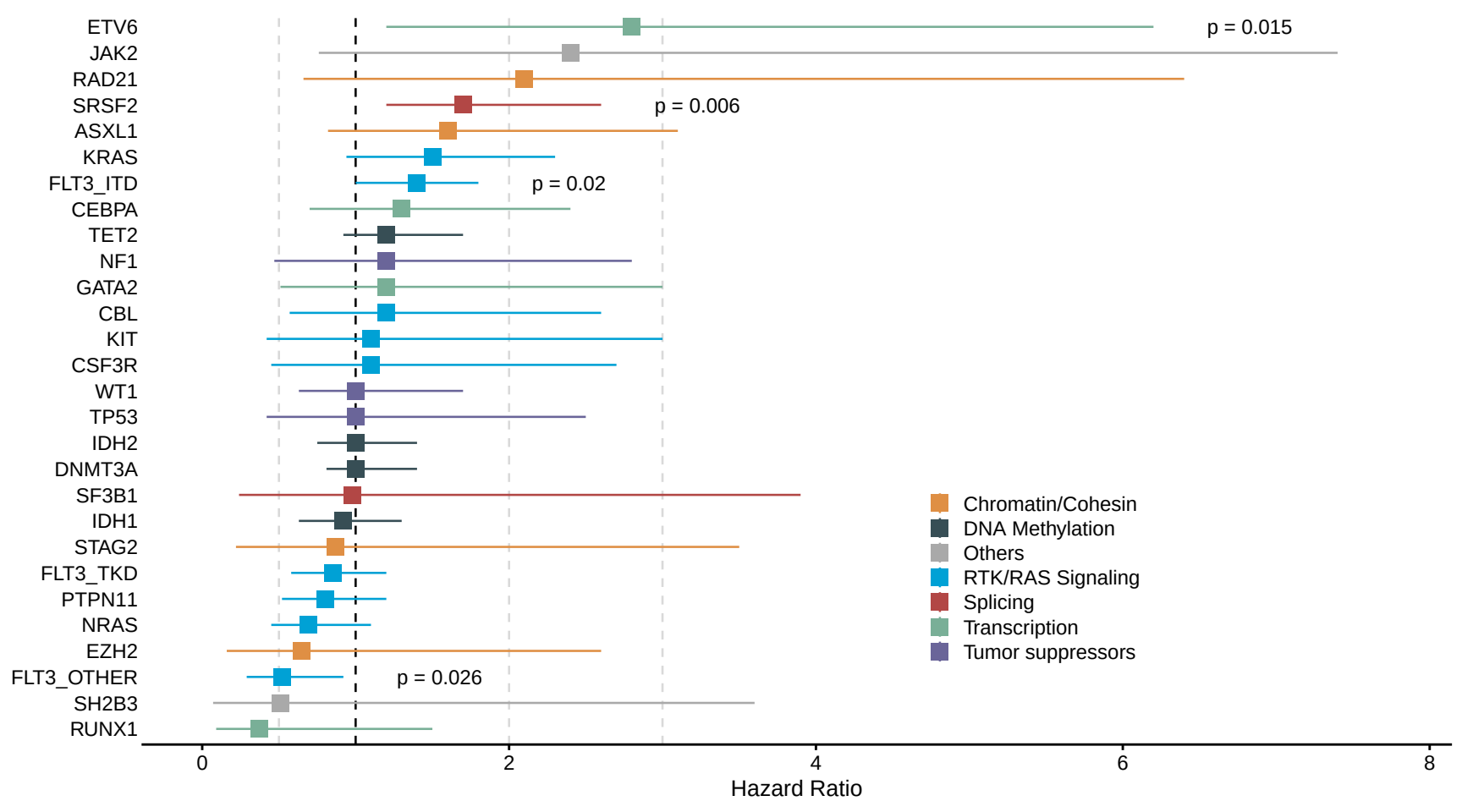
ETV6
JAK2
RAD21
SRSF2
ASXL1
KRAS
FLT3_ITD
CEBPA
TET2
NF1
GATA2
CBL
KIT
CSF3R
WT1
TP53
IDH2
DNMT3A
SF3B1
IDH1
STAG2
FLT3_TKD
PTPN11
NRAS
EZH2
FLT3_OTHER
SH2B3
RUNX1
p = 0.015
p = 0.006
p = 0.02
p = 0.026
Chromatin/Cohesin
DNA Methylation
Others
RTK/RAS Signaling
Splicing
Transcription
Tumor suppressors
0
2
4
6
8
Hazard Ratio

A

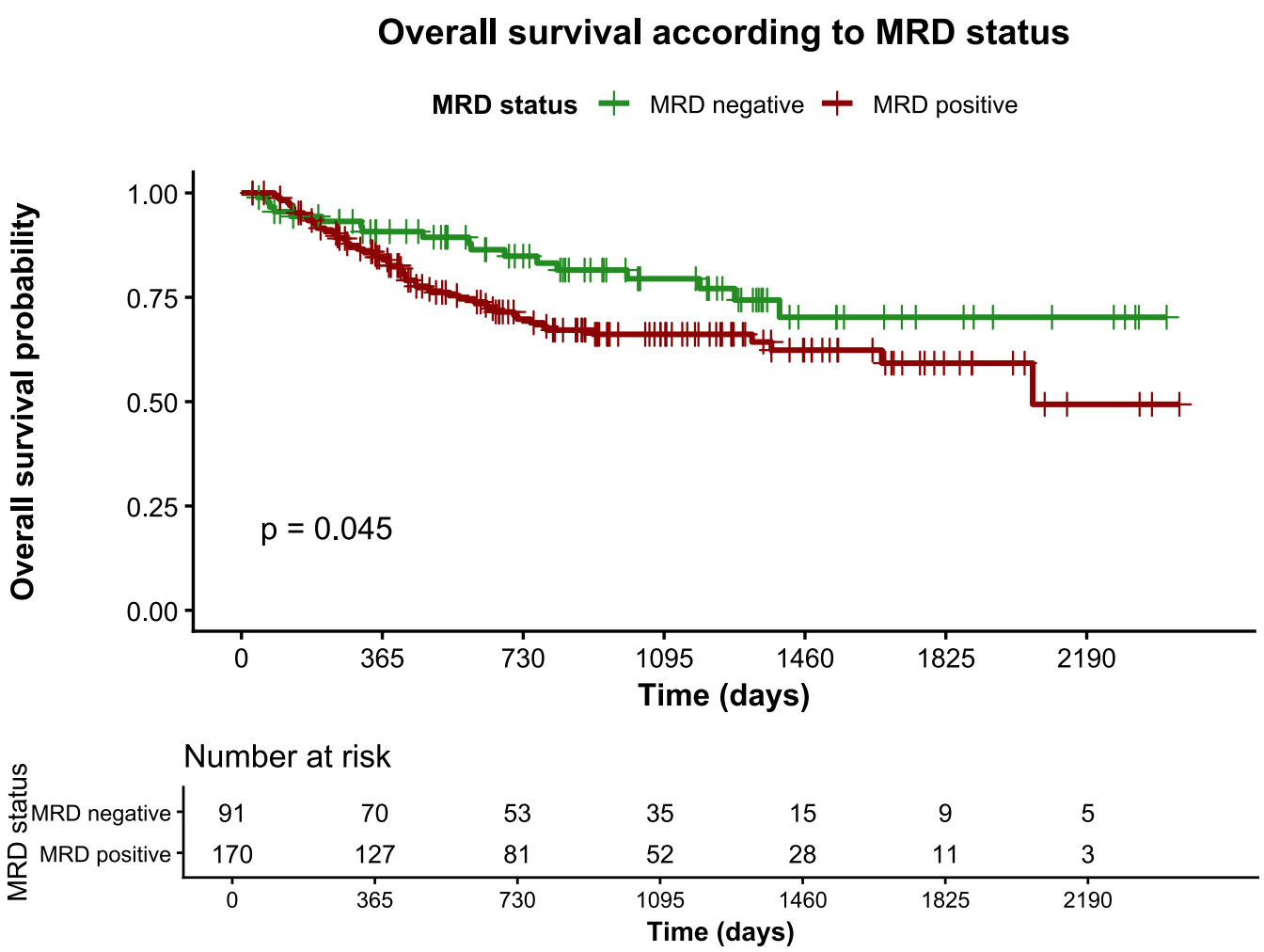
Overall survival according to MRD status
MRD status
MRD negative
MRD positive
Overall survival probability
1.00
0.75
0.50
0.25
0.00
p = 0.045
0
365
730
1095
1460
1825
2190
Time (days)
Number at risk
MRD status
MRD negative 91 70 53 35 15 9 5
MRD positive 170 127 81 52 28 11 3
0
365
730
1095
1460
1825
2190
Time (days)

B

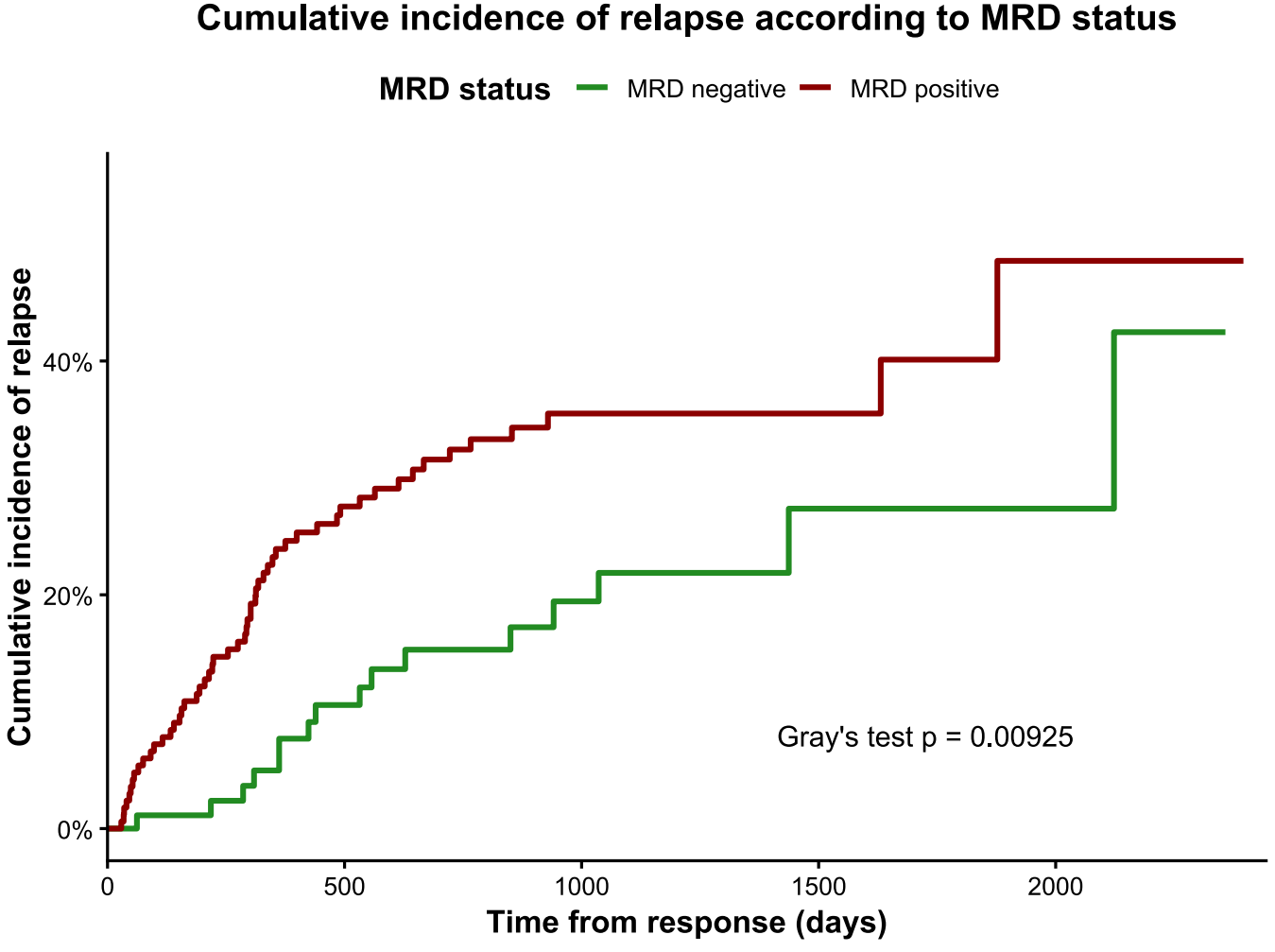
Cumulative incidence of relapse according to MRD status
MRD status
MRD negative
MRD positive
Cumulative incidence of relapse
40%
20%
0%
Gray's test p = 0.00925
0
500
1000
1500
2000
Time from response (days)

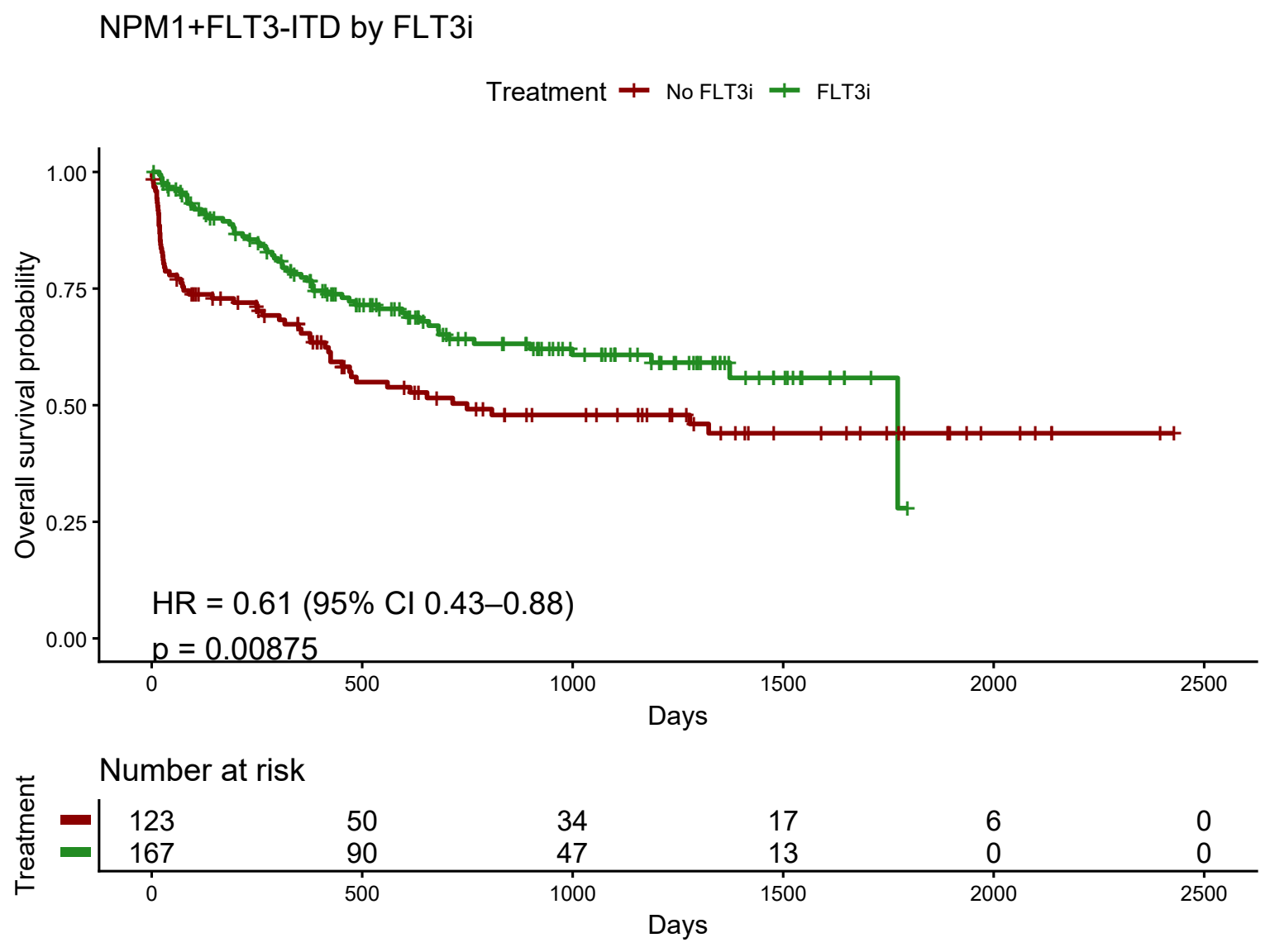
NPM1+FLT3-ITD by FLT3i
Treatment
No FLT3i
FLT3i
Overall survival probability
1.00
0.75
0.50
0.25
0.00
HR = 0.61 (95% CI 0.43–0.88)
p = 0.00875
0
500
1000
1500
2000
2500
Days
Number at risk
Treatment
123
50
34
17
6
0
167
90
47
13
0
0
0
500
1000
1500
2000
2500
Days

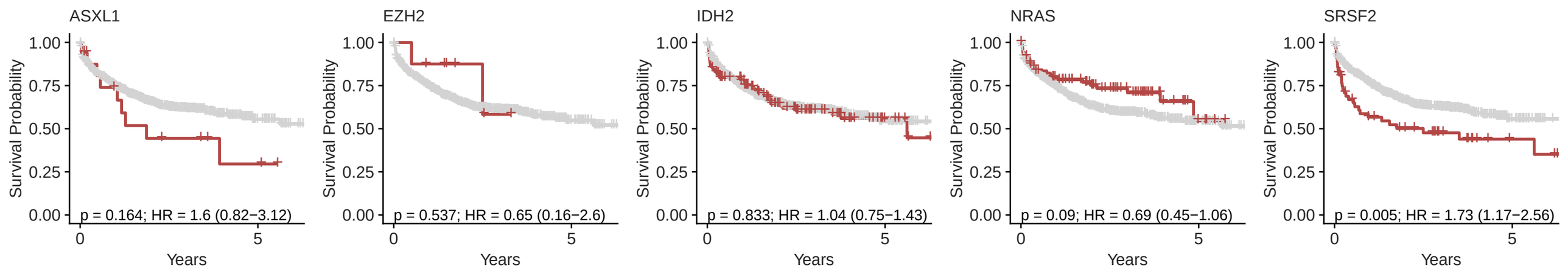
ASXL1
p = 0.164; HR = 1.6 (0.82−3.12)
EZH2
p = 0.537; HR = 0.65 (0.16−2.6)
IDH2
p = 0.833; HR = 1.04 (0.75−1.43)
NRAS
p = 0.09; HR = 0.69 (0.45−1.06)
SRSF2
p = 0.005; HR = 1.73 (1.17−2.56)
CBL
p = 0.608; HR = 1.22 (0.57−2.58)
FLT3_ITD
p = 0.02; HR = 1.36 (1.05−1.77)
JAK2
p = 0.126; HR = 2.37 (0.76−7.41)
PTPN11
p = 0.311; HR = 0.8 (0.52−1.23)
STAG2
p = 0.845; HR = 0.87 (0.22−3.5)
Survival Probability
1.00
0.75
0.50
0.25
0.00
0
5
Years

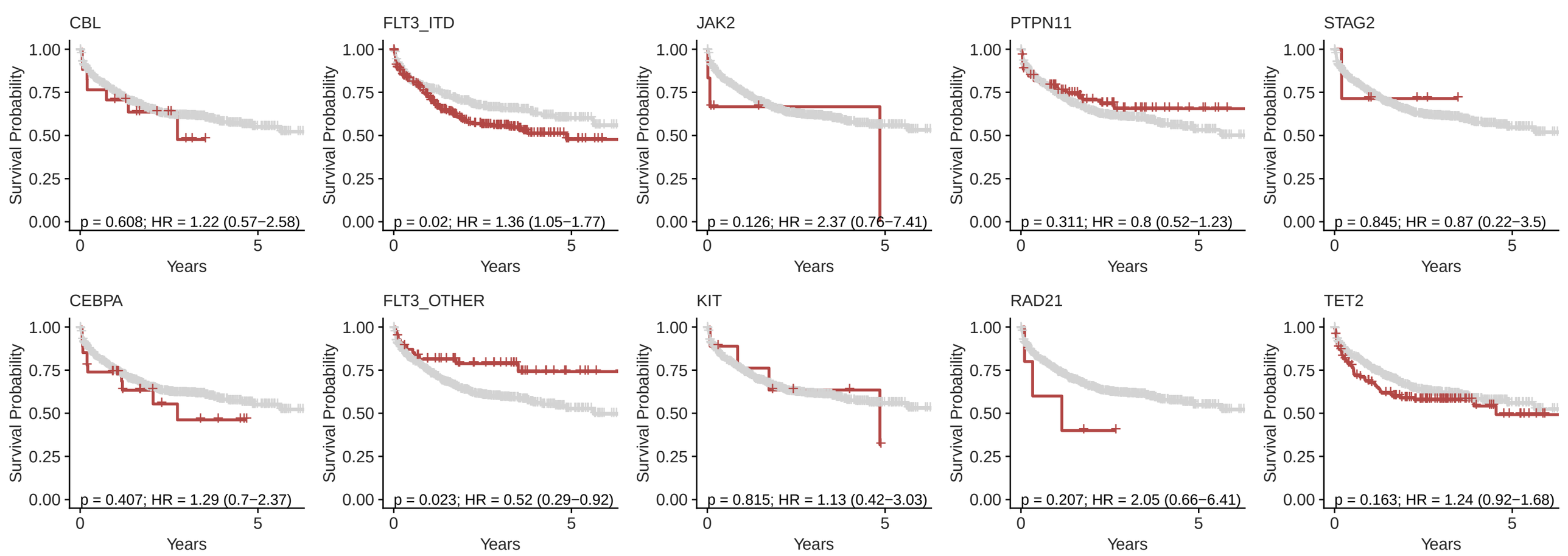
CEBPA
p = 0.407; HR = 1.29 (0.7−2.37)
FLT3_OTHER
p = 0.023; HR = 0.52 (0.29−0.92)
KIT
p = 0.815; HR = 1.13 (0.42−3.03)
RAD21
p = 0.207; HR = 2.05 (0.66−6.41)
TET2
p = 0.163; HR = 1.24 (0.92−1.68)
CSF3R
p = 0.841; HR = 1.09 (0.45−2.66)
FLT3_TKD
p = 0.403; HR = 0.85 (0.58−1.24)
KRAS
p = 0.085; HR = 1.48 (0.94−2.32)
RUNX1
p = 0.141; HR = 0.37 (0.09−1.47)
TP53
p = 0.978; HR = 1.01 (0.42−2.46)
Survival Probability
1.00
0.75
0.50
0.25
0.00
0
5
Years

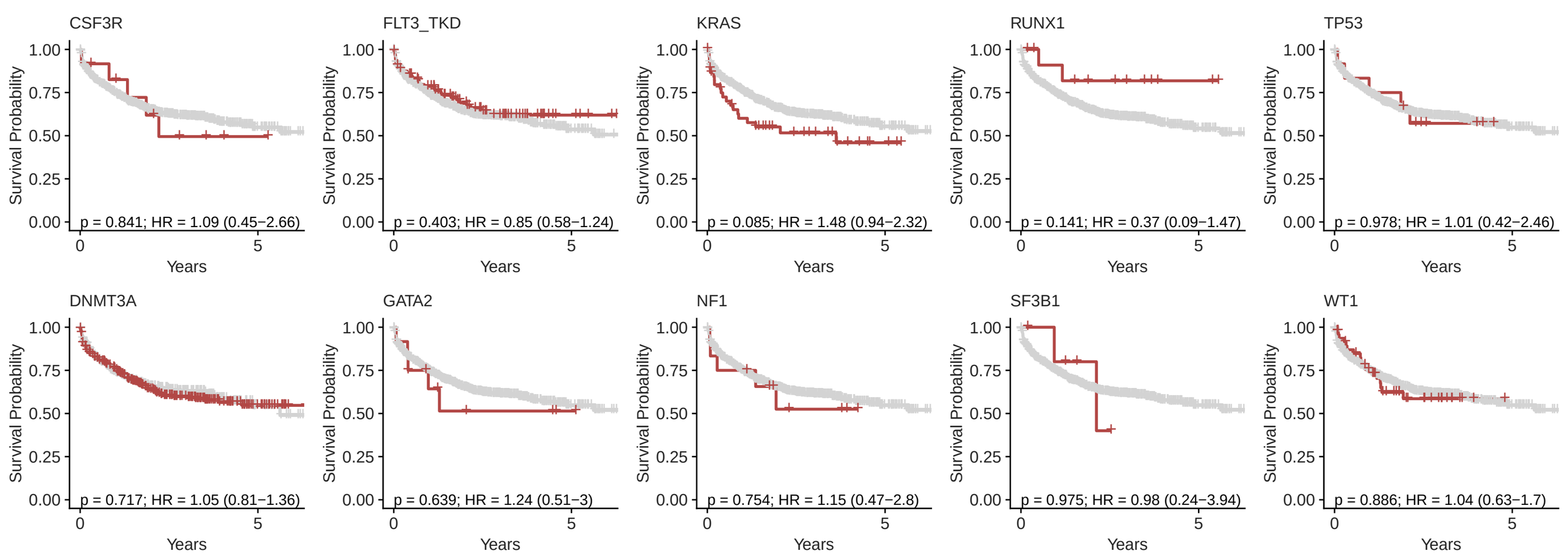
DNMT3A
p = 0.717; HR = 1.05 (0.81−1.36)
GATA2
p = 0.639; HR = 1.24 (0.51−3)
NF1
p = 0.754; HR = 1.15 (0.47−2.8)
SF3B1
p = 0.975; HR = 0.98 (0.24−3.94)
WT1
p = 0.886; HR = 1.04 (0.63−1.7)
ETV6
p = 0.011; HR = 2.75 (1.22−6.2)
IDH1
p = 0.647; HR = 0.92 (0.63−1.34)
NPM1
p = 1; HR = NA (NA−NA)
SH2B3
p = 0.487; HR = 0.51 (0.07−3.6)
Survival Probability
1.00
0.75
0.50
0.25
0.00
0
5
Years

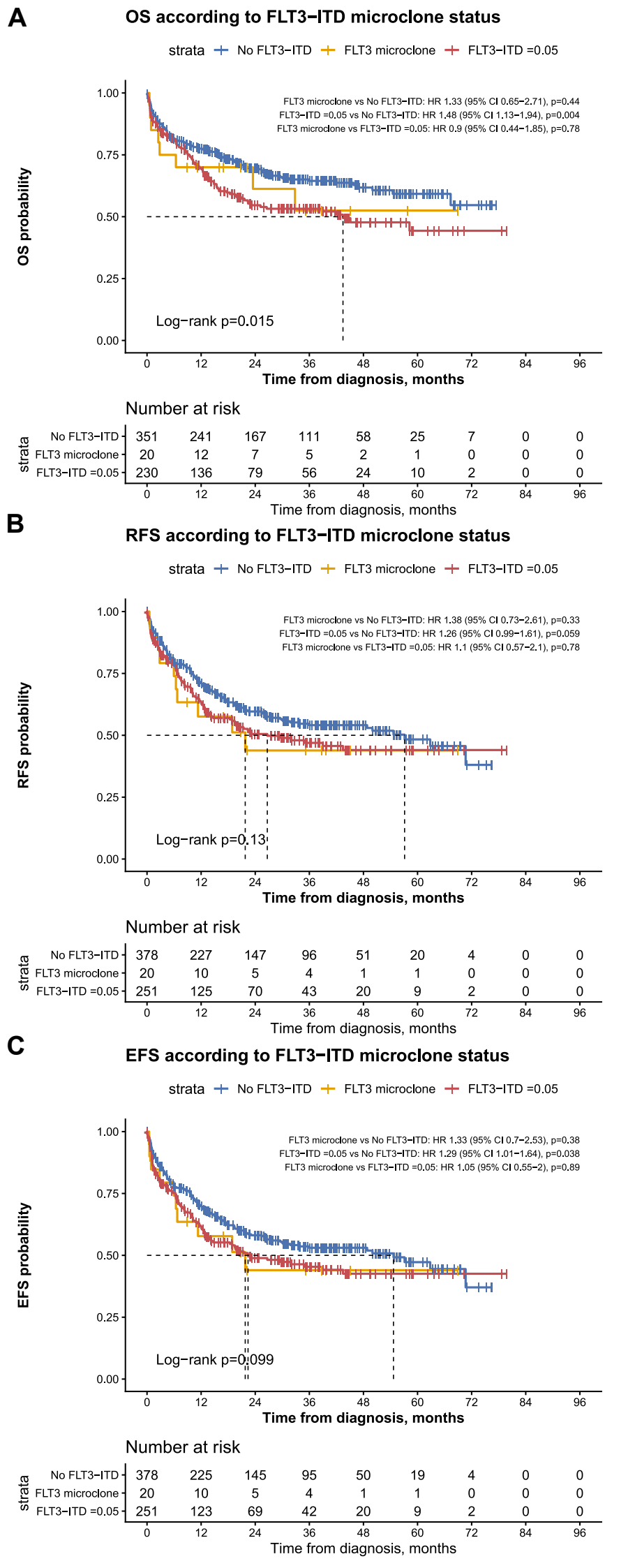
A
OS according to FLT3−ITD microclone status
strata No FLT3−ITD FLT3 microclone FLT3−ITD =0.05
FLT3 microclone vs No FLT3−ITD: HR 1.33 (95% CI 0.65−2.71), p=0.44
FLT3−ITD =0.05 vs No FLT3−ITD: HR 1.48 (95% CI 1.13−1.94), p=0.004
FLT3 microclone vs FLT3−ITD =0.05: HR 0.9 (95% CI 0.44−1.85), p=0.78
OS probability
1.00
0.75
0.50
0.25
0.00
Log−rank p=0.015
0 12 24 36 48 60 72 84 96
Time from diagnosis, months
Number at risk
strata
No FLT3−ITD 351 241 167 111 58 25 7 0 0
FLT3 microclone 20 12 7 5 2 1 0 0 0
FLT3−ITD =0.05 230 136 79 56 24 10 2 0 0
0 12 24 36 48 60 72 84 96
Time from diagnosis, months
B
RFS according to FLT3−ITD microclone status
strata No FLT3−ITD FLT3 microclone FLT3−ITD =0.05
FLT3 microclone vs No FLT3−ITD: HR 1.38 (95% CI 0.73−2.61), p=0.33
FLT3−ITD =0.05 vs No FLT3−ITD: HR 1.26 (95% CI 0.99−1.61), p=0.059
FLT3 microclone vs FLT3−ITD =0.05: HR 1.1 (95% CI 0.57−2.1), p=0.78
RFS probability
1.00
0.75
0.50
0.25
0.00
Log−rank p=0.13
0 12 24 36 48 60 72 84 96
Time from diagnosis, months
Number at risk
strata
No FLT3−ITD 378 227 147 96 51 20 4 0 0
FLT3 microclone 20 10 5 4 1 1 0 0 0
FLT3−ITD =0.05 251 125 70 43 20 9 2 0 0
0 12 24 36 48 60 72 84 96
Time from diagnosis, months
C
EFS according to FLT3−ITD microclone status
strata No FLT3−ITD FLT3 microclone FLT3−ITD =0.05
FLT3 microclone vs No FLT3−ITD: HR 1.33 (95% CI 0.7−2.53), p=0.38
FLT3−ITD =0.05 vs No FLT3−ITD: HR 1.29 (95% CI 1.01−1.64), p=0.038
FLT3 microclone vs FLT3−ITD =0.05: HR 1.05 (95% CI 0.55−2), p=0.89
EFS probability
1.00
0.75
0.50
0.25
0.00
Log−rank p=0.099
0 12 24 36 48 60 72 84 96
Time from diagnosis, months
Number at risk
strata
No FLT3−ITD 378 225 145 95 50 19 4 0 0
FLT3 microclone 20 10 5 4 1 1 0 0 0
FLT3−ITD =0.05 251 123 69 42 20 9 2 0 0
0 12 24 36 48 60 72 84 96
Time from diagnosis, months

Single MR-gene mutation vs all

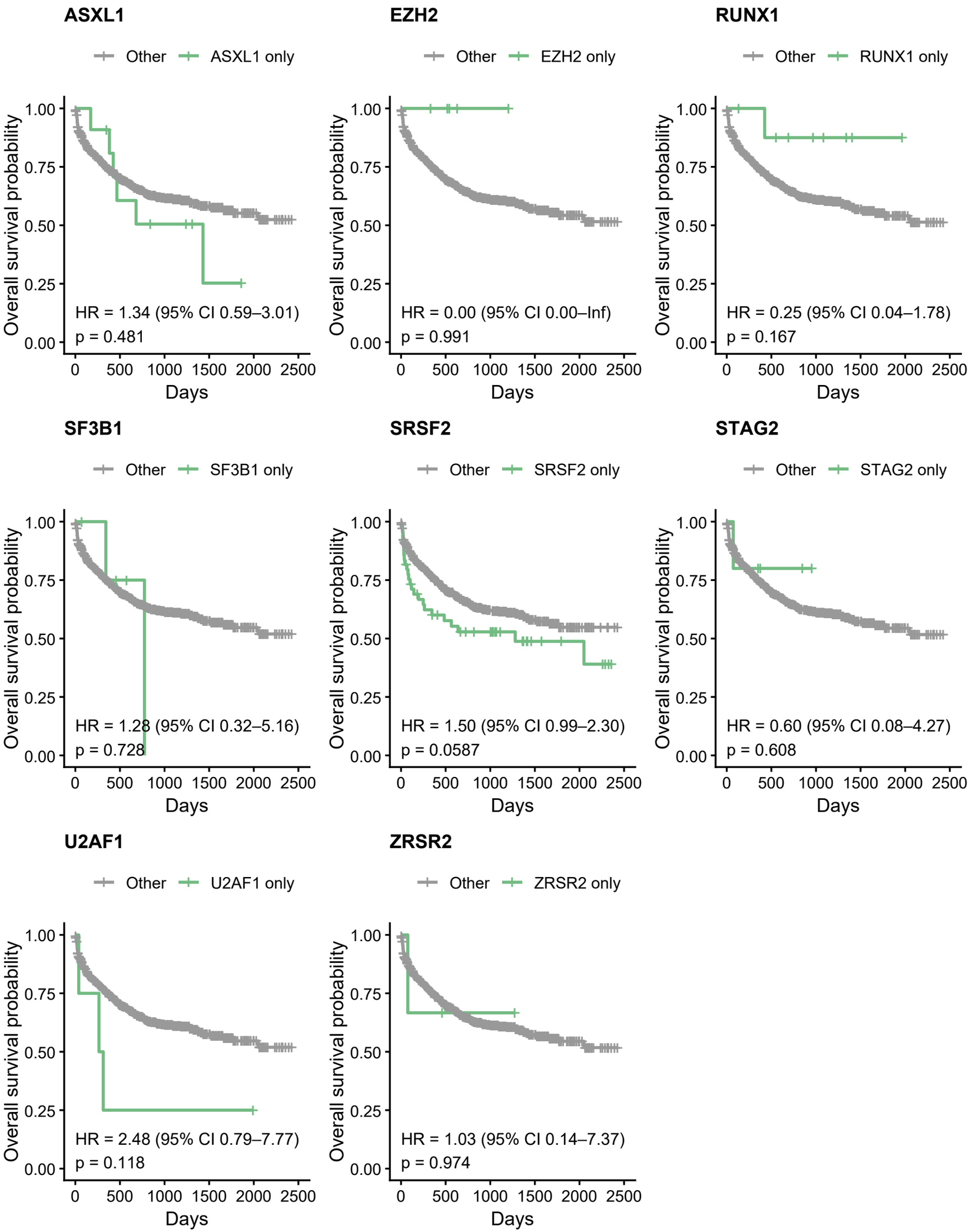

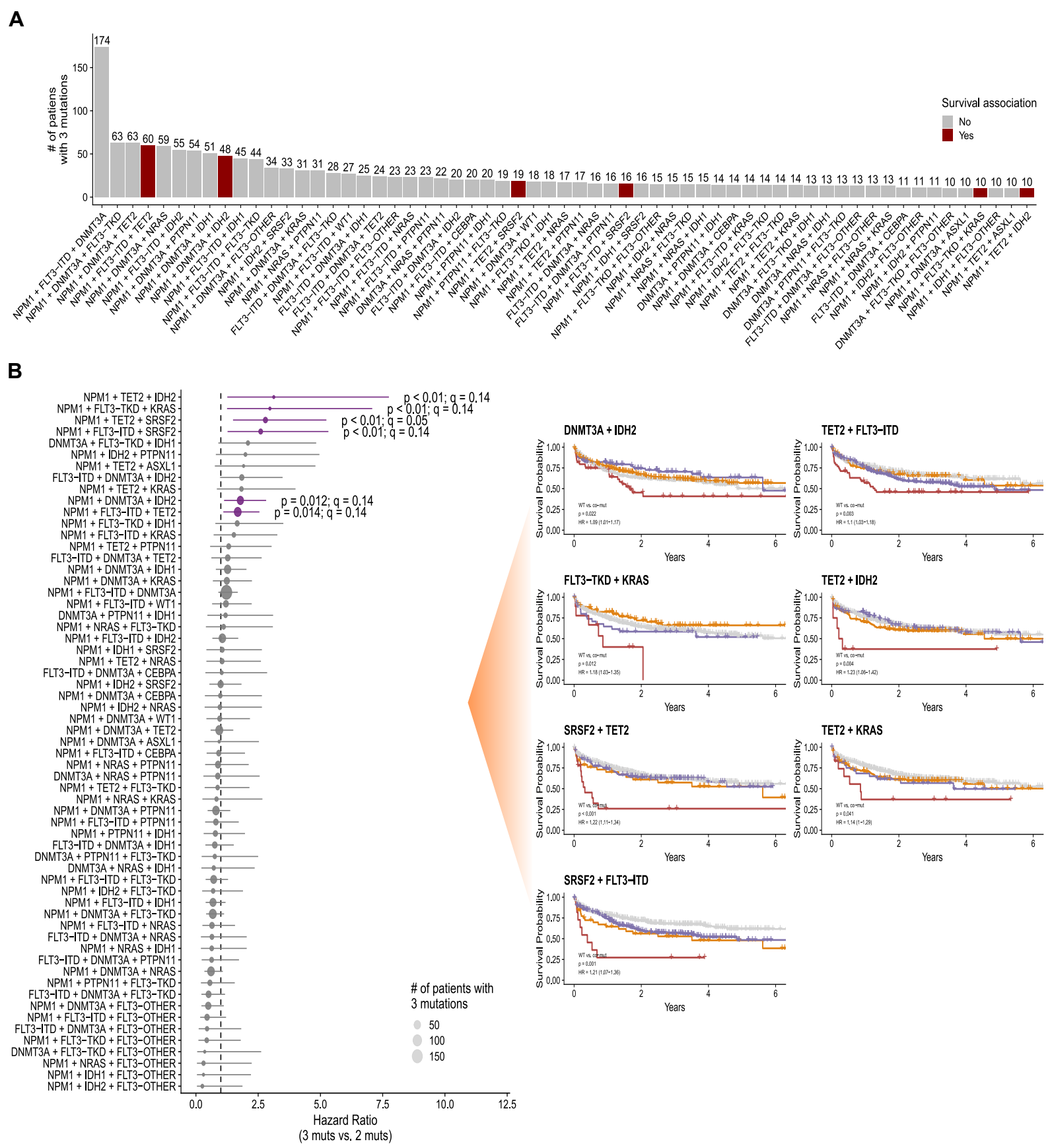
A
# of patiens with 3 mutations
Survival association
No
Yes
B
p < 0.01; q = 0.14
p < 0.01; q = 0.14
p < 0.01; q = 0.05
p < 0.01; q = 0.14
p = 0.012; q = 0.14
p = 0.014; q = 0.14
# of patients with 3 mutations
Hazard Ratio
(3 muts vs. 2 muts)
DNMT3A + IDH2
TET2 + FLT3−ITD
FLT3−TKD + KRAS
TET2 + IDH2
SRSF2 + TET2
TET2 + KRAS
SRSF2 + FLT3−ITD
Survival Probability
Years

A

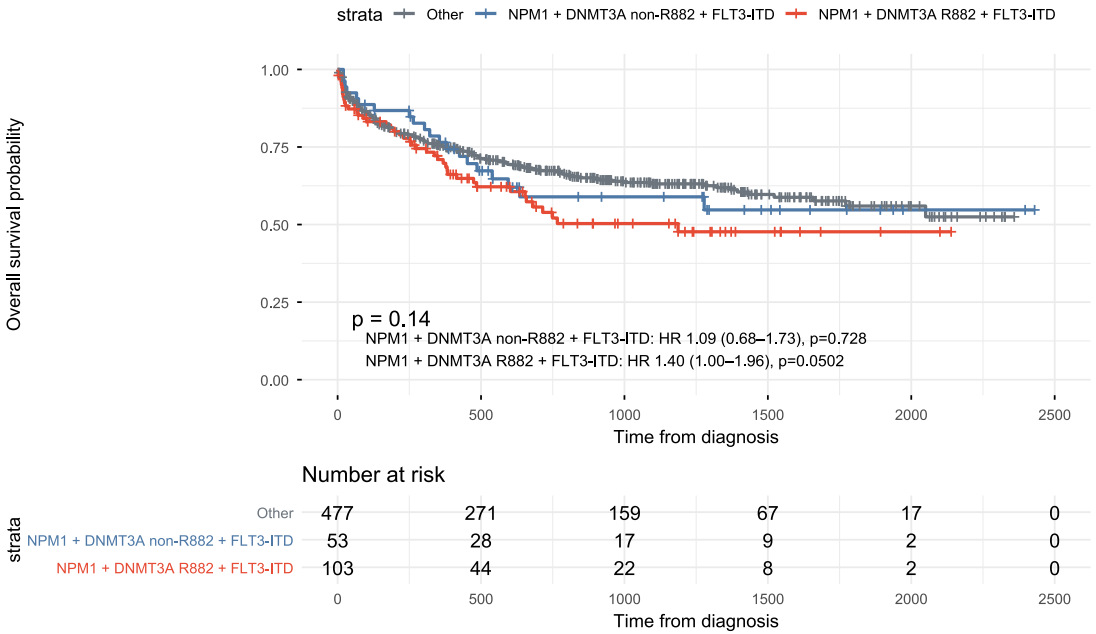
strata
Other
NPM1 + DNMT3A non-R882 + FLT3-ITD
NPM1 + DNMT3A R882 + FLT3-ITD
Overall survival probability
1.00
0.75
0.50
0.25
0.00
p = 0.14
NPM1 + DNMT3A non-R882 + FLT3-ITD: HR 1.09 (0.68–1.73), p=0.728
NPM1 + DNMT3A R882 + FLT3-ITD: HR 1.40 (1.00–1.96), p=0.0502
0
500
1000
1500
2000
2500
Time from diagnosis
Number at risk
strata
Other 477 271 159 67 17 0
NPM1 + DNMT3A non-R882 + FLT3-ITD 53 28 17 9 2 0
NPM1 + DNMT3A R882 + FLT3-ITD 103 44 22 8 2 0
0
500
1000
1500
2000
2500
Time from diagnosis

B

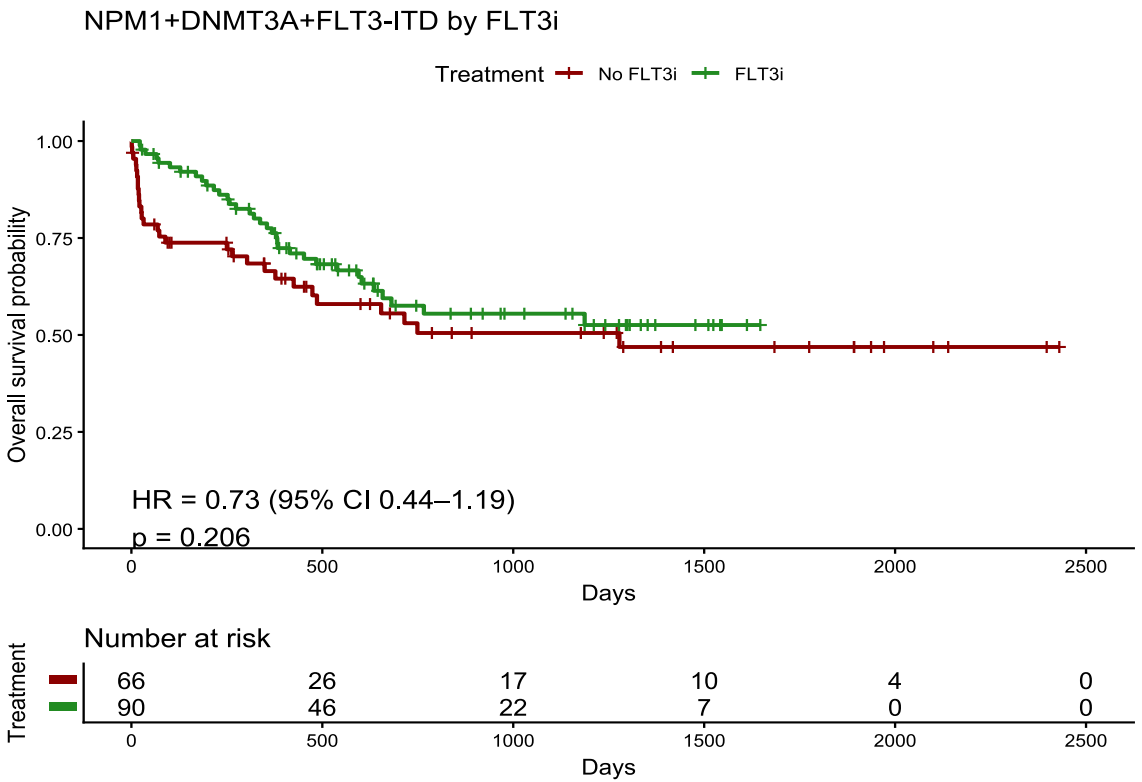
NPM1+DNMT3A+FLT3-ITD by FLT3i
Treatment
No FLT3i
FLT3i
Overall survival probability
1.00
0.75
0.50
0.25
0.00
HR = 0.73 (95% CI 0.44–1.19)
p = 0.206
0
500
1000
1500
2000
2500
Days
Number at risk
Treatment
66 26 17 10 4 0
90 46 22 7 0 0
0
500
1000
1500
2000
2500
Days